A dynamic network model of the unsecured interbank lending market

Blasques, Francisco; Bräuning, Falk; Lelyveld, Iman van

published in
Journal of Economic Dynamics and Control
2018

DOI (link to publisher)
10.1016/j.jedc.2018.03.015

document version
Publisher's PDF, also known as Version of record

Journal of Economic Dynamics & Control 90 (2018) 310–342

Contents lists available at ScienceDirect

Journal of Economic Dynamics & Control

journal homepage: www.elsevier.com/locate/jedc

A dynamic network model of the unsecured interbank lending market

Francisco Blasques[a], Falk Bräuning[b,*], Iman van Lelyveld[a,c]

[a] VU University Amsterdam and Tinbergen Institute, De Boelelaan 1105, Amsterdam 1081 HV, The Netherlands
[b] Federal Reserve Bank of Boston, 600 Atlantic Avenue, Boston, MA 02210, United States
[c] De Nederlandsche Bank, Westeinde 1, Amsterdam 1017 ZN, The Netherlands

ARTICLE INFO

Article history:
Received 14 June 2017
Revised 22 March 2018
Accepted 28 March 2018
Available online 3 April 2018

JEL classification:
C33
C51
E52
G01
G21

Keywords:
Interbank liquidity
Financial networks
Credit-risk uncertainty
Monitoring
Trading relationships
Indirect inference estimation

ABSTRACT

We introduce a dynamic network model of interbank lending and estimate the parameters by indirect inference using network statistics of the Dutch interbank market from February 2008 to April 2011. We find that credit-risk uncertainty and peer monitoring are significant factors in explaining the sparse core-periphery structure of the market and the presence of relationship lending. Shocks to credit-risk uncertainty lead to extended periods of low market activity, intensified by reduced peer monitoring. Moreover, changes in the central bank's interest rate corridor have both a direct effect on the market as well as an indirect effect by changing banks' monitoring efforts.

1. Introduction

The global financial crisis of 2007–2008 highlighted the crucial role of interbank lending markets, both in the financial system and the real economy. In particular, after Lehman Brothers collapsed in September 2008, increased uncertainty in the banking system led to severe distress in unsecured interbank lending markets. As a result, monetary policy implementation was hampered and credit supply to the nonfinancial sector declined substantially, with adverse consequences for both the financial sector and the real economy. In order to mitigate these adverse effects, central banks intervened by injecting additional liquidity into the banking sector and by adjusting their monetary policy instruments. As a consequence, central banks became the primary intermediaries for large parts of the money market during the crisis (Cœuré, 2013).

Generally, having a central counterparty for an unsecured interbank market reduces contagion effects through bilateral credit exposures (Allen and Gale, 2000). Likewise, search frictions resulting from asymmetric information about the liquidity positions of other banks are mitigated. On the other hand, with a central counterparty, private information that banks have

* Corresponding author.
E-mail address: Falk.Braeuning@bos.frb.org (F. Bräuning).

https://doi.org/10.1016/j.jedc.2018.03.015
0165-1889/

about the credit risk posed by other banks is no longer reflected in the price at which banks can obtain funds. Moreover, the incentives for banks to acquire and process such information are largely eliminated. Indeed, as Rochet and Tirole (1996) argue, the operation of a decentralized interbank lending market must be motivated by the benefits of peer monitoring.[1]

Our paper contributes to this debate by introducing and estimating a dynamic network model to analyze the role of credit-risk uncertainty and peer monitoring in the unsecured interbank lending market. The key economic drivers of the model's outcomes are asymmetric information about counterparty risk and liquidity conditions elsewhere in the market. In particular, our model focuses on the role that peer monitoring plays in reducing bank-to-bank credit-risk uncertainty and that endogenous counterparty selection (directed counterparty search) plays in mitigating search frictions resulting from the over-the-counter market structure.

An important novelty of this paper is the econometric analysis of our model. Given the complex model structure, we estimate the network model with an indirect inference estimator (Gourieroux et al., 1993) based on auxiliary statistics that are taylored to characterize the structure of trading relationships in the interbank lending network. Specifically, our indirect inference estimator is based on an auxiliary vector that contains network statistics (for example, density, reciprocity, and centrality) that have become popular in characterizing the topological structure of interbank markets (see, for instance, Bech and Atalay, 2010). We further complement these network statistics with moment statistics of bilateral interest rates and volumes, and measures of bilateral lending relationships. Our indirect inference estimator is then obtained as the parameter that minimizes the distance between the auxiliary vectors obtained from observed data and from data simulated from the model. To show the econometric validity of our estimation, we analyze asymtotic properties, sensitivity of auxiliary statistics, and the estimator's small-sample behavior (under both correct model specification and when the data generating process differs from the imposed model structure). In addition, we discuss the impact of potential identification failure. Both the sensitivity analysis and the Monte Carlo study of the finite-sample distribution suggest that the estimator does not suffer from identification problems.

We then use the indirect inference procedure to estimate our network model from transaction-level data on unsecured overnight loans made among the 50 largest Dutch banks between mid-February 2008 through April 2011. Our estimation results show that peer monitoring aligned with endogenous counterparty selection generates an amplification mechanism that lies at the core of our estimated model: Lending banks invest in monitoring those borrowers whom they expect to be profitable, either because of large loan volumes, high expected returns on granted loans, or because of a high frequency of borrowing contacts. Borrowing banks obtain part of the surplus generated by peer monitoring, which strengthens their relationship with the lending bank. As a consequence of this monitoring, uncertainty about credit risk is reduced, more loans are granted, and lender banks further increase their monitoring efforts in expectation of greater profits. Thus, monitoring efforts have a multiplier effect that has important implications for the endogenous network structure as well as for the amplification of shocks to credit-risk uncertainty and changes in monetary policy.

First, we find that peer monitoring, search frictions, and uncertainty about counterparty risk assume significant roles when matching the observed trading network's topology—notably, its high sparsity, low reciprocity, and skewed degree distribution. In particular, the estimated model implies a tiered network structure (core-periphery structure) that can be explained in part by banks' heterogeneous liquidity shocks.[2] However, comparing the estimated model with a calibrated model that omits monitoring (but holds everything else equal) and with a restricted estimation shows that credit-risk uncertainty and peer monitoring are crucial in reinforcing the network's core-periphery structure: large money center banks are more intensively monitored by their lenders, and they in turn closely monitor their borrowers, leading to both lower bid and offer rates, as well as fueling their role as market intermediaries. Our analysis shows that this multiplier effect is also necessary to generate stability in the core-periphery structure as well as in bilateral trading relationships (as well the impact that relationship lending has on interest rates) similar to that observed in the data.

Second, our dynamic analysis reveals that adverse shocks to credit-risk uncertainty can suppress market activity for extended periods of time. The lending network shrinks because bilateral interest rates increase as a response to the higher perceived counterparty risk. Hence, interbank lending becomes less profitable relative to using the outside options (the central bank's lending and deposit facilities), and recourse to the standing facilities replaces a number of trades. Moreover, in response to the shock and in expectation of higher uncertainty in the future, associated with lower profitability, banks invest less in peer monitoring. Negative feedback loops between lower levels of peer monitoring and search amplify this reduction, thereby preventing a faster market recovery. We also find that after the adverse shock, the lending network becomes less interconnected and more concentrated among a few banks (larger reciprocity and more skewed degree distribution) as those banks with extensive trading relationships stay in the market. In particular, bank pairs that face low bank-to-bank

[1] The European Central Bank (ECB) highlights the role of peer monitoring and private information as well: "Specifically, in the unsecured money markets, where loans are uncollateralised, interbank lenders are directly exposed to losses if the interbank loan is not repaid. This gives lenders incentives to collect information about borrowers and to monitor them over the lifetime of the interbank loan.... Therefore, unsecured money markets play a key peer monitoring role." See the speech by Benoât Cœuré, Member of the Executive Board of the ECB, at the Morgan Stanley 16th Annual Global Investment seminar, Tourrettes, Provence, June 16, 2012. http://www.ecb.europa.eu/press/key/date/2012/html/sp120616.en.html, retrieved October 10, 2013.

[2] Banks in the core are highly interconnected and typically have a structural liquidity deficit (investment opportunity) but large variances in liquidity shocks. On the other hand, peripheral banks almost exclusively trade with the core banks and typically have a structural funding surplus and experience small-scale shocks.

credit-risk uncertainty (due to private information acquired through previous monitoring) continue to lend to each other and, as a consequence, the average interest rate spread of granted loans decreases during the crisis period.

Third, the analysis of the estimated model shows that the central bank's interest rate corridor (the interest rate spread between its lending and deposit facilities) is a crucial determinant of interbank lending activity. In particular, we find that by increasing the corridor width, the central bank fosters interbank lending by directly reducing the attractiveness of the outside options, thereby increasing the potential surplus obtainable from bilateral interbank lending. However, we also document an indirect multiplier effect: since the increased expected surplus from interbank trading intensifies banks' monitoring and search efforts, these in turn act to further improve credit conditions and credit availability in the market, leading to more liquidity and a more efficient market usage. Moreover, we find that in response to an increase in the central bank's corridor width, the interbank lending network destabilizes as more loans are settled outside of established relationships (spot lending increases).

The paper is structured as follows. Section 2 discusses the related literature. Section 3 introduces the economic model. Section 4 provides details on the estimation procedure, discusses the model's parameter estimates, and analyzes the relative fit in terms of various criteria. Section 5 analyzes the estimated model and studies policy implications, while Section 6 concludes.

2. Stylized facts and related literature

Interbank lending networks exhibit two stylized facts. First, interbank markets exhibit a sparse core-periphery structure whereby a few highly interconnected core banks account for most of the observed trades. Peripheral banks have a low number of counterparties and almost exclusively trade with core banks.[3] Second, interbank lending is based on stable bilateral trading relationships that facilitate access to credit and offer better loan conditions.[4] By explaining these two stylized facts using a model based on credit-risk uncertainty and peer monitoring, our paper is related to several strands of the literature.

First, the basic economic forces driving the proposed interbank lending model are credit-risk uncertainty, peer monitoring, and search frictions. Thereby, our paper is related to recent work by Afonso and Lagos (2015), who propose a search model to explain intraday trading dynamics in the spirit of over-the-counter models such as Duffie et al. (2005). Like these authors, we also build our dynamic model on bilateral bargaining and search frictions. However, Afonso and Lagos (2015) abstract from the role of bank default that was introduced by Bech and Monnet (2013). Neither model accounts for credit-risk uncertainty nor focuses on explaining the network structure of interbank markets and the endogenous formation of trading relationships. Moreover, since these models assume a continuum of atomistic agents where the probability of two banks being matched repeatedly is zero, there is no role for the emergence of long-term trading relationships.

On the other hand, building on the classical banking model of Diamond and Dybvig (1983), Freixas and Holthausen (2005), Freixas and Jorge (2008), and Heider et al. (2015) have focused on the role that asymmetric information about counterparty risk plays in the allocation of liquidity. In particular, Heider et al. (2015) show that informational frictions can lead to adverse selection and a market freeze with liquidity hoarding. In these models, however, interbank markets are anonymous and competitive, and hence the models abstract from the actual over-the-counter (OTC) structure where deals are negotiated on a bilateral basis and the realized credit conditions depend on heterogeneous expectations both about counterparty risk and credit conditions. The role of peer monitoring and private information that we consider a key driver of interbank lending has been highlighted by Rochet and Tirole (1996) and Furfine (2001).

Second, our paper is related to the growing literature on how financial networks are formed (see, for example, Babus, 2013; Farboodi, 2014; Gale and Kariv, 2007; in 't Veld et al., 2014; Vuillemey and Breton, 2014).[5] In particular, Babus (2013) shows that when agents trade risky assets over-the-counter, asymmetric information and costly link formation can endogenously lead to an undirected star network with just one intermediary. Farboodi (2014) develops a model that generates a core-periphery structure in which banks try to capture intermediation rents. Crucially, her model relies on the assumption that there are differences in investment opportunities (see also in 't Veld et al., 2014). Our model confirms the importance of this type of bank heterogeneity for the emergence of a core-periphery structure, but credit-risk uncertainty and peer monitoring are the key drivers of persistent bilateral lending relationships that reinforce the core-periphery structure. In contrast to these studies that are concerned with the emergence of a static network, our paper also analyzes the lending network's dynamic behavior.

Third, our paper contributes to the econometric analysis of structural network models, in particular, parameter estimation. Most of the existing literature of empirical network analysis has largely relied on reduced-form statistical models (e.g.,

[3] For empirical evidence on the topological structure of interbank markets see, for instance, Soramäki et al. (2007), May et al. (2008), and Bech and Atalay (2010) for the United States; Boss et al. (2004) for Austria; Iori et al. (2008) and Lux and Fricke (2012) for Italy; Becher et al. (2008) for the United Kingdom; Craig and von Peter (2014) for Germany; in 't Veld and van Lelyveld (2014) for the Netherlands, and Anand et al. (2018) for a cross-country study.

[4] The existence of interbank relationship lending has been documented by, among others, Furfine (1999), Furfine (2001), Ashcraft and Duffie (2007), and Afonso et al. (2013) for the United States; Iori et al. (2008), Affinito (2012) for Italy; Cocco et al. (2009) for Portugal; and Bräuning and Fecht (2017) for Germany.

[5] The effects of the network structure on financial contagion has been studied, for instance, by Georg (2013), Gai et al. (2011), Acemoglu et al. (2015), and Gofman (2014). We do not focus on contagion effects in this paper.

Hoff et al., 2002; Kolaczyk, 2009; Snijders et al., 2010), We show how descriptive network statistics can be used in an indirect inference procedure to learn about structural parameters in complex network models; see Grazzini et al. (2014) for a discussion of the challenges of these kinds of models.[6] Our estimation results contribute to recent empirical studies on the drivers of interbank lending markets. For the U.S. Afonso et al. (2011) provide evidence that concerns about counterparty risk play a larger role than liquidity hoarding (Acharya and Merrouche, 2013) around Lehman Brothers' bankruptcy. The dynamics of our estimated model confirm that shocks to counterparty-risk uncertainty can reduce lending activity for extended periods of time that are also accompanied by a more concentrated lending network. In this latter respect, Gabrieli and Georg (2014) provide empirical evidence on the network shrinkage in the euro money market during the financial crisis.

Finally, our paper is related to the literature on the conduct of monetary policy in a corridor system (e.g., Berentsen and Monnet, 2008; Poole, 1968; Whitesell, 2006). Our paper extends this literature by analyzing the effects of changes in the interest rate corridor on the structure of the lending network and the cross-sectional distribution of interest rates. In particular, our model suggests that increasing the corridor width incentivizes peer monitoring and private interbank lending. However, absent a view on the central bank's preferences, we cannot make statements about the optimal corridor width (cf. Berentsen and Monnet, 2008; Bindseil and Jabłecki, 2011).

3. The interbank network model

We model the interbank lending market as a network consisting of N nodes with a time-varying number of directed links between them. Each node represents a bank and each link represents an unsecured interbank loan that is characterized by a loan amount and an interest rate. Time periods are indexed by $t \in \mathbb{N}$. Banks are indexed by i or j, with $i, j \in \{1, \dots, N\}$.

Each period, banks are subject to positive or negative liquidity shocks that affect the daily operations of their payment accounts (for example, clients that want to make payments). Banks wish to smooth these shocks by borrowing and lending unsecured funds from each other using an OTC market. An option outside the interbank lending market exists, as banks have unlimited access to the central bank's standing facilities with deposit rate $\underline{r}$ and lending rate $\bar{r}$ with $\bar{r} \geq \underline{r}$.[7]

Banks enter the interbank market with the objective of lending and borrowing funds to maximize expected discounted profits by: *(i)* choosing which banks to approach for bilateral Nash bargaining about interest rates, and *(ii)* setting bilateral monitoring expenditures to mitigate *uncertainty* about counterparty credit risk.

In the following subsections, we discuss the model's structure, solve for banks' optimal dynamic monitoring and search decisions, and specify an adaptive expectation mechanism to derive the model's reduced form.

3.1. Counterparty-risk uncertainty

Borrowing banks may default on interbank loans and—due to the unsecured nature of interbank lending—impose losses on lenders. Bank j's *true probability of default* at time t is denoted by $P_{j,t}$ and is derived as the tail probability of a random variable $z_{j,t}$ that measures the *true financial distress* of bank j,

$$P_{j,t} := \mathbb{P}(z_{j,t} > \epsilon).$$

In particular, $z_{j,t}$ is constructed so that bank j is forced into default whenever $z_{j,t}$ takes values above some common time-invariant threshold $\epsilon > 0$. This threshold can be interpreted as either a minimum regulatory requirement or a level that seems sufficient to operate in the market. We focus on the case when $z_{j,t}$ is identically and independently distributed (*iid*) for each bank j with $\mathbb{E}(z_{j,t}) = 0$ and $\sigma^2 = \mathrm{Var}(z_{j,t})$, such that there is no cross-section or time heterogeneity in banks' true default probability.

Asymmetric information about counterparty risk (the riskiness and liquidity of a borrower's assets) is seen as a major characteristic of financial crises that leads to inefficient allocations in money markets (Heider et al., 2015).[8] Our focus is on the *uncertainty* about counterparty credit risk that underpins the interbank lending network structure and drives its dynamics. Asymmetric information problems arise because counterparty risk assessment is not based on the true default risk but merely on the *perceived probability of default* that bank i attributes to bank j at time t. This probability is denoted by $P_{i,j,t}$ and is obtained as the tail probability of a random variable $z_{i,j,t}$ that measures bank i's *perceived financial distress* of bank j. The perceived financial distress $z_{i,j,t}$ is based on the true financial distress $z_{j,t}$ but contains an added component of bank-to-bank uncertainty that is modeled by the addition of an independent *perception error* $e_{i,j,t}$ so that

$$z_{i,j,t} = z_{j,t} + e_{i,j,t},$$

[6] A recent attempt to calibrate a network model is presented by Gofman (2014), who matches the density, the maximum degree, and the number of intermediaries with those of the federal funds market, as reported by Bech and Atalay (2010).

[7] This paper focuses on banks' liquidity management and does not consider asset-liability allocation problems other than those associated with interbank lending and resorting to the central bank's facility.

[8] In this respect, William Dudley, President and CEO of the Federal Reserve Bank of New York, remarked: "So what happens in a financial crisis? First, the probability distribution [representing a creditor's assessment of the value of a financial firm] shifts to the left as the financial environment deteriorates.... Second, and even more importantly, the dispersion of the probability distribution widens—lenders become more uncertain about the value of the firm.... A lack of transparency in the underlying assets will exacerbate this increase in dispersion." ("More Lessons from the Crisis", November 13, 2009), see http://www.bis.org/review/r091117a.pdf.

where $e_{i,j,t}$ is a random variable distributed according to some density, with $\mathbb{E}(e_{i,j,t}) = 0$ and $\mathrm{Var}(e_{i,j,t}) = \tilde{\sigma}^2_{i,j,t}$. The perception error introduces bank-to-bank-specific assessments about the counterparty credit risk posed by the same borrower, bank j. That is, different banks may form different risk perceptions about the same borrower.

Since the exact distribution of the perception error $e_{i,j,t}$ is unknown to bank i, every bank is assumed to approximate the tail probability of the extreme event of default by the conservative bound provided by Chebyshev's one-tailed inequality,[9]

$$\mathbb{P}(z_{i,j,t} > \epsilon) \leq \frac{\sigma^2_{i,j,t}}{\sigma^2_{i,j,t} + \epsilon^2} = \frac{\sigma^2 + \tilde{\sigma}^2_{i,j,t}}{\sigma^2 + \tilde{\sigma}^2_{i,j,t} + \epsilon^2} =: P_{i,j,t}.$$

Hence, both the bank's true risk profile and the additional uncertainty resulting from the perception error increase the perceived probability of default, which lender banks use to make their credit-risk assessment. The asymmetric information problem (characterized by a strictly positive perception-error variance $\sigma^2_{i,j,t}$) drives a wedge between the perceived probability of default and the true probability of default, even under the assumption that the perception error has a mean of zero.

The evolution of the perception-error variance $\tilde{\sigma}^2_{i,j,t}$ is determined by the knowledge that bank i has about bank j's default risk. This knowledge depends on factors such as the pair's past trading history and, in particular, the monitoring expenditure that bank i allocates to learning about bank j's financial situation (the monitoring is discussed in more detail in the following section). Specifically, we assume that the bank-to-bank uncertainty $\tilde{\sigma}^2_{i,j,t}$ evolves over time according to autoregressive dynamics given by

$$\log \tilde{\sigma}^2_{i,j,t+1} = \alpha_\sigma + \gamma_\sigma \log \tilde{\sigma}^2_{i,j,t} + \beta_\sigma \phi_{i,j,t} + \delta_\sigma u_{i,j,t}, \tag{1}$$

where $\alpha_\sigma \in \mathbb{R}$, $\gamma_\sigma \in (0, 1)$, $\beta_\sigma \geq 0$, and $\delta_\sigma > 0$ are parameters; $\phi_{i,j,t}$ is a function of past bilateral trading intensity and the monitoring cost that measures the amount of *new information* that bank i collects about the financial situation of bank j in period t; $u_{i,j,t} \sim \mathcal{N}(0, 1)$ is an *iid* shock to the counterparty-risk uncertainty. Moreover, we impose the restriction that $\beta_\sigma \leq 0$, and hence the added information gathered through monitoring and past interaction (weakly) reduces the perception-error variance. Due to the log specification, $\tilde{\sigma}^2_{i,j,t}$ follows a nonlinear process $\tilde{\sigma}^2_{i,j,t+1} = \xi_{i,j,t}(\phi_{i,j,t}, \tilde{\sigma}^2_{i,j,t}) = \xi(\phi_{i,j,t}, \tilde{\sigma}^2_{i,j,t}, u_{i,j,t})$. Further, we can derive $\frac{\partial \xi_{i,j,t}}{\partial \phi_{i,j,t}} < 0$ and $\frac{\partial^2 \xi_{i,j,t}}{\partial \phi^2_{i,j,t}} > 0$, and hence our model dictates that there are decreasing returns to scale in information gathering.

Eq. (1) is at the core of our model, as it determines the time-variation and cross-sectional heterogeneity in the bank-to-bank-specific perceived probabilities of default $P_{i,j,t}$. Conditional on these bank-to-bank perceived probabilities of defaults, banks negotiate the loan conditions.

3.2. Bargaining and equilibrium interest rates

In the OTC interbank market, bank pairs bilaterally negotiate the specific loan terms. In the following description of the bargaining process, without loss of generality, let bank i be the potential lender bank that has a liquidity surplus and bank j be the potential borrower bank that has a liquidity deficit. From the viewpoint of bank i, lending funds to bank j at time t at a given bilateral equilibrium interest rate $r_{i,j,t}$ is a risky investment with a stochastic return,

$$R_{i,j,t} = \begin{cases} r_{i,j,t} & \text{with probability } 1 - P_{i,j,t} \\ -1 & \text{with probability } P_{i,j,t}, \end{cases}$$

where we assume that given a default, the loss is 100%. We further assume that bank i is risk neutral and maximizes its expected lending profit conditional on the perceived probability of default $P_{i,j,t}$. The expected profit per euro is given by

$$\bar{R}_{i,j,t} := \mathbb{E}_t R_{i,j,t} = (1 - P_{i,j,t}) r_{i,j,t} - P_{i,j,t},$$

where $\mathbb{E}_t$ denotes the expected value with respect to the perceived default probabilities. The expected surplus that lender bank i obtains from lending to borrower j is based on the difference between $\bar{R}_{i,j,t}$ and $\underline{r}$, the outside option for lenders (the interest rate for depositing funds at the central bank's standing facilities), but takes into account that this difference only goes to lender bank i if it is not in default. If it is in default (with true probability $P_{i,t}$) any cash flow is transferred to the liquidator. Hence, the expected surplus (including expected default) of lender i when lending to borrower j is given by $(1 - P_{i,t})(\bar{R}_{i,j,t} - \underline{r})$.

For the borrower bank j, the cost per euro when borrowing from lender bank i is simply given by the equilibrium interest rate $r_{i,j,t}$. The expected surplus relative to $\bar{r}$, the outside option for borrowing from the central bank's lending facility, takes

[9] Instead of the Chebyshev bound, one can assume that the banks use a certain distribution to compute this probability. In this case, we just have to use the respective cumulative distribution function.

into account the true probability that bank j will default and is given by $(1-P_{j,t})(\bar{r}-r_{i,j,t})$.[10] Note that we implicitly assume that when lender bank i defaults, a solvent borrower j will still have to repay the principal and interest to the liquidator.

We follow the standard approach and assume that banks negotiate interest rates bilaterally and agree on the generalized Nash bargaining solution (see, for instance, Afonso and Lagos, 2015; Bech and Klee, 2011 for similar applications to interbank markets). Written in terms of surplus relative to the outside option, the bilateral equilibrium interest rate between lender i and borrower j at time t then satisfies

$$r_{i,j,t} \in \arg\max_{\tilde{r}} \Big((1-P_{i,t})\big((1-P_{i,j,t})\tilde{r} - P_{i,j,t} - \underline{r}\big) \Big)^{\theta} \Big((1-P_{j,t})(\bar{r}-\tilde{r}) \Big)^{1-\theta},$$

where the outside options for lenders ($\underline{r}$) and borrowers ($\bar{r}$) satisfy $\bar{r} \geq \underline{r}$. The parameter $\theta \in [0, 1]$ denotes the bargaining power of lender i relative to borrower j. As the exchange of funds is voluntary, the bilateral Nash bargaining problem is subject to the participation constraints $r_{i,j,t} \leq \bar{r}$ and $\bar{R}_{i,j,t} \geq \underline{r}$, and hence the central bank's interest rate corridor sets the upper and lower bounds for the interbank lending rates. We specifically use the Nash bargaining as a computational feasible way to model bargaining under asymmetric information. The Nash solution might in this case, for example, be interpreted as the lender (the uninformed player here) making a take-it or leave-it offer to the borrower.[11]

Normalizing $\underline{r} = 0$ and denoting $\bar{r} = r$, as well as ignoring the multiplicative factors, the corresponding bilateral equilibrium interest rate satisfies equivalently $r_{i,j,t} \in \arg\max_{\tilde{r}} \big((1-P_{i,j,t})\tilde{r} - P_{i,j,t}\big)^{\theta} \big((1-P_{j,t})(r-\tilde{r})\big)^{1-\theta}$, which we solve to obtain

$$r_{i,j,t} = \theta r + (1-\theta)\frac{P_{i,j,t}}{1-P_{i,j,t}}, \tag{2}$$

where the last term is a risk premium depending on the perceived default probability, $P_{i,j,t}$, that reflects the potential principal loss. The minimum interest rate that lender i is willing to accept is $r^{min}_{i,j,t} = P_{i,j,t}/(1-P_{i,j,t})$, which is obtained from setting $\mathbb{E}_t R_{i,j,t}$ equal to the return of the outside option. Similarly, the borrower will not accept rates higher than $r^{max}_{i,j,t} = r$. Importantly, when the perceived default probability is sufficiently high, it is possible that the rate at which a bank is willing to lend is higher than the rate that the central bank charges for using its lending facility. In such circumstances, banks will not trade with each other, and borrowers will turn to the central bank instead of using the interbank market. In fact, it is possible that the interbank market disappears if lending is perceived to be too risky.

Using the definition of the perceived probability $P_{i,j,t}$, we can rewrite the bilateral equilibrium interest rate as a function of the default threshold, the true financial distress variance, and the variance of the perception error as

$$r_{i,j,t} = \theta r + (1-\theta)\frac{\sigma^2 + \tilde{\sigma}^2_{i,j,t}}{\epsilon^2}.$$

Taking the partial derivatives of this function gives $\frac{\partial r_{i,j,t}}{\partial \sigma} = \frac{(1-\theta)2\sigma}{\epsilon^2} > 0$ and $\frac{\partial^2 r_{i,j,t}}{\partial \sigma^2} = \frac{2(1-\theta)}{\epsilon^2} > 0$, and similarly $\frac{\partial r_{i,j,t}}{\partial \tilde{\sigma}_{i,j,t}} = \frac{(1-\theta)2\tilde{\sigma}_{i,j,t}}{\epsilon^2} > 0$ and $\frac{\partial^2 r_{i,j,t}}{\partial \tilde{\sigma}^2_{i,j,t}} = \frac{2(1-\theta)}{\epsilon^2} > 0$. Thus, the equilibrium interest rate increases with the uncertainty about counterparty risk. Note also that the second derivative is the same, so that the bilateral interest rate exhibits the same curvature in both dimensions.

The partial derivative of the expected return with respect to the perception-error variance is $\frac{\partial \bar{R}_{i,j,t}}{\partial \tilde{\sigma}^2_{i,j,t}} = -\frac{\partial P_{i,j,t}}{\partial \tilde{\sigma}^2_{i,j,t}} + \frac{\partial 1-P_{i,j,t}}{\partial \tilde{\sigma}^2_{i,j,t}} r_{i,j,t} + (1-P_{i,j,t})\frac{\partial r_{i,j,t}}{\partial \tilde{\sigma}^2_{i,j,t}} = -\frac{\epsilon(1+r)\theta}{(\epsilon^2+\sigma^2+\tilde{\sigma}^2_{i,j,t})^2} < 0$. These terms show the channels through which increasing uncertainty about counterparty risk affects the expected return. First, increasing uncertainty about counterparty risk decreases $\bar{R}_{i,j,t}$ as $\frac{\partial P_{i,j,t}}{\partial \tilde{\sigma}^2_{i,j,t}} > 0$; hence loss due to default becomes more likely. Second, increasing uncertainty about counterparty risk increases the risk premium that is obtained if the borrower survives. However, the net effect is negative and thus the expected return decreases for a larger perception-error variance.

The preceding analysis reveals that the bilateral equilibrium interest rate under the asymmetric information problem, here parametrized by the perception-error variance, is not Pareto efficient. Indeed, we can compute the interest rate and

[10] In the model, all banks have unlimited recourse to the central bank's standing facilities (specifically to the marginal lending facility) at any point in time. Thereby, we implicitly assume that all banks have sufficient collateral to back these operations (the euro area's national central banks provide liquidity under the marginal lending facility either as overnight repurchase agreements or as overnight collateralized loans). Moreover, holding the required collateral imposes a zero cost for all agents. At the margin, the central bank does not price banks' borrowing, as it assesses banks' riskiness as a sunk cost.

[11] In contrast to search models such as Afonso and Lagos (2015), our bilateral bargaining solution is derived under the assumption that the outside option for each loan is always the central bank's standing facilities. In contrast, in search models where two agents from a continuous population are randomly paired and allowed to bargain the terms of trade, each agent's outside options are determined by the expected future trading opportunities that may arise in the market. For our purpose of estimating a structural network model with endogenous counterparty selection, this approach is computationally infeasible, as the costs of obtaining the outside options (computing the value function) for our high dimensional problem are prohibitive in our simulation-based estimation procedure. In contrast to Afonso and Lagos (2015), our bilateral bargaining problem also incorporates an expected return, as the borrower may default on the loan and be unable to repay the principal amount to the lender; see also the bargaining problem in Bech and Monnet (2013).

expected return for the perfect information case where $\tilde{\sigma}^2_{i,j,t} = 0$ (denoted by $r^{PI}_{i,j,t}$ and $\bar{R}^{PI}_{i,j,t}$, where the superscript *PI* stands for the perfect information case) and compare it with the asymmetric information case,

$$r_{i,j,t} - r^{PI}_{i,j,t} = \frac{(1-\theta)\tilde{\sigma}^2_{i,j,t}}{\epsilon^2} > 0 \quad \text{and} \quad \bar{R}^{PI}_{i,j,t} - \bar{R}_{i,j,t} = \frac{\epsilon^2(1+r)\theta\tilde{\sigma}^2_{i,j,t}}{(\epsilon^2+\sigma^2)(\epsilon^2+\sigma^2+\tilde{\sigma}^2_{i,j,t})} > 0,$$

which gives the total reduction in (expected) surplus per euro of the loan due to the asymmetric information problem. This loss of surplus depends positively on the perception-error variance $\tilde{\sigma}^2_{i,j,t}$, which may be reduced by banks' peer monitoring efforts, as discussed in the next subsection.

3.3. Monitoring, counterparty selection and transaction volumes

Banks can engage in costly peer monitoring targeted at mitigating asymmetric information problems about counterparty risk. Therefore, let $m_{i,j,t} \in \mathbb{R}^+_0$ denote the expenditure that bank i incurs in period t for monitoring bank j. The *added information* that bank i acquires about bank j in period t is a linear function of the monitoring expenditure in period t and a loan, $l_{i,j,t} \in \{0, 1\}$, from bank i to bank j, enacted during trading session t,

$$\phi_{i,j,t} = \phi(m_{i,j,t}, l_{i,j,t}) = \beta_\phi + \beta_{1,\phi} m_{i,j,t} + \beta_{2,\phi} l_{i,j,t}. \tag{3}$$

The added information affects the perception-error variance in future periods (see Eq. (1)). By allowing $\phi_{i,j,t}$ to be a function of both the loan indicator $l_{i,j,t}$ and monitoring efforts $m_{i,j,t}$, we distinguish between (costly) active information acquisition, such as creditworthiness checks, and freely obtained information, such as trust, built through repeated interactions. Monitoring efforts only affect the information about borrower risk, which influences the uncertainty about counterparty risk (the asymmetric information problem).[12]

Due to the OTC structure of interbank markets, bilateral Nash bargaining between any banks i and j in the market occurs only if these two banks have established contact. Therefore, we introduce a binary variable $B_{i,j,t}$ that indicates if bank i and j are connected at time t, so that bargaining as described in the previous subsection is possible. Specifically, we model $B_{i,j,t}$ as a Bernoulli random variable with success probability $\lambda_{i,j,t}$ that can be influenced by the search efforts of bank j directed toward lender i,

$$B_{i,j,t} \sim \text{Bernoulli}(\lambda_{i,j,t}) \text{ with } \lambda_{i,j,t} = \frac{1}{1+\exp(-\beta_\lambda(s_{j,i,t} - \alpha_\lambda))}, \tag{4}$$

where $s_{j,i,t} \in \mathbb{R}^+_0$ captures the search cost incurred by bank j (which has a liquidity deficit) when approaching lender i in period t. Hence, we assume loans are borrower-initiated in the sense that banks with a liquidity deficit approach potential lender banks for bargaining. Moreover, we impose the conditions that $\beta_\lambda > 0$ and $\alpha_\lambda > 0$. For $\beta_\lambda \to \infty$ this function converges to a step function that corresponds to a deterministic link formation at fixed cost α_λ. For $s_{j,i,t} = 0$, we still have $\lambda_{i,j,t} > 0$, so even with no search costs there is still a positive probability that contact occurs, allowing for bargaining and a transfer of funds from bank i to bank j. Our modeling choice of search costs reflects a cost-per-contact notion (e.g., for each deal, money market traders devoting their time and resources to contacting traders at other banks).

Once two banks establish contact and bilateral Nash bargaining about the interest rate is successful, interbank lending takes place. The amount of the granted loan $y_{i,j,t}$ is exogenously given by a nonlinear transformation of two random variables that follow a lender-bank and borrower-bank-specific distribution,

$$y_{i,j,t} = \min\{\zeta^i_{i,j,t}, -\zeta^j_{i,j,t}\}\mathbb{I}(\zeta^i_{i,j,t} > 0)\mathbb{I}(\zeta^j_{i,j,t} < 0), \tag{5}$$

where the random variable $\zeta^i_{i,j,t} \in \mathbb{R}$ can be interpreted as bank i's liquidity shock (superscript i) realized at the time the transaction occurs between bank i and j. The transaction-specific liquidity shocks cannot be used for transactions with other banks in the same (or subsequent) period but must be smoothed instantaneously with the central bank or the respective counterparty at hand.[13]

---

[12] Because we are interested in the role of monitoring on credit-risk uncertainty as the main driving force behind the observed interbank network structure and its dynamics, we deliberately focus only on this channel of monitoring and abstract from endogenous feedback effects between monitoring and risk-taking that also affect the true default probability (which is exogenously given in our model).

[13] This modeling choice follows the idea that upon contact each (ordered) pair of banks can exchange a stochastic pair-specific amount of funds which is exogenously determined by a (transaction-specific) realization from their (bank-specific) liquidity shock distributions. As a consequence of this modeling choice, a lender bank i may have several loans with different counterparties during the same time period ($\Sigma_j l_{i,j,t} > 1$). Moreover, lender bank i may also be borrowing during the same time period ($\Sigma_j l_{i,j,t} > 0$ and $\Sigma_k l_{k,i,t} > 0$) such that intermediation may arise where some banks act as both borrower and lender in the market (see Craig and von Peter, 2014). Furthermore, reciprocal lending relationships within one period may occur ($l_{i,j,t} = l_{j,i,t} = 1$). In a previous version of the paper, we assumed a different sampling scheme similarly to Babus (2013) and Vuillemey and Breton (2014) where at each instance each bank is paired with at most one counterparty (for example, pairing two banks randomly at each instance). For a given observed data frequency (in our daily analysis), we then aggregate the simulated data to a lower frequency to allow for nodes with multiple links. The sampling scheme we employ can be seen as a computationally less costly shortcut to sampling at a higher frequency.

We allow for bank-level heterogeneity of liquidity shocks and assume that $\zeta^i_{i,j,t}$ is independently and normally distributed with the bank-specific mean μ_{ζ^i} and variance $\sigma^2_{\zeta^i}$ parameters such that

$$\zeta^i_{i,j,t}|\mu_{\zeta^i},\sigma^2_{\zeta^i} \overset{iid}{\sim} \mathcal{N}(\mu_{\zeta^i},\sigma^2_{\zeta^i}), \quad \text{where} \quad \mu_{\zeta^i} \sim \mathcal{N}(\mu_\mu,\sigma^2_\mu) \quad \text{and} \quad \log\sigma_{\zeta^i} \sim \mathcal{N}(\mu_\sigma,\sigma^2_\sigma),$$

and we allow for correlation between μ_{ζ^i} and $\sigma^2_{\zeta^i}$ through the parameter $\rho_\zeta := \text{Corr}(\mu_{\zeta^i},\sigma_{\zeta^i})$. For convenience, we assume (conditional) independence and normality of liquidity shocks, as this allows us to analytically compute part of the model's solution. This simple type of heterogeneity in the distribution of banks' liquidity shocks allows us to model size effects related to the scale of banks' businesses through larger variances that are drawn from a log–normal distribution. Moreover, this assumption allows us to account for structural liquidity provision or demand by some banks through a nonzero mean $\mu_{\zeta_{i,t}}$. The parameter ρ_ζ allows both effects to be correlated; for instance, some banks on average might supply small amounts of liquidity to the market (for example deposit-collecting institutions).

To keep track of all the loans in the interbank network, we formally define the binary link variable $l_{i,j,t}$ that indicates if an interbank loan between lending bank i and borrowing bank j at time t is granted (the extensive margin of credit) as

$$l_{i,j,t} = \begin{cases} 1 & \text{if } B_{i,j,t} = 1 \wedge r_{i,j,t} \leq r \wedge y_{i,j,t} > 0 \\ 0 & \text{otherwise.} \end{cases} \tag{6}$$

Hence, an established contact is only a necessary condition for a successful interbank loan to take place: upon a contact being made, funds are transferred if and only if the bargaining process is successful.[14]

Finally, since the volume of a granted loan $y_{i,j,t}$ is exogenously determined, matching is only affected by bank j's search efforts, while for a sufficiently good risk assessment, the interest rate bank i offers is only directly affected by its monitoring efforts. Thus, we abstract from credit rationing on the intensive margin of credit (that is, lender banks reduce the amount of loans that they grant in response to an increase in perceived counterparty risk).

3.4. Profit maximization, optimal monitoring, and search

Each bank $i \in \{1,\dots,N\}$ faces the dynamic problem of allocating resources to monitor its counterparties and to choose which bank to transact with in order to maximize the expected discounted payoffs from interbank lending and borrowing net of search and monitoring costs. Formally, the infinite-horizon dynamic optimization problem of each bank is given by

$$\max_{\{m_{i,j,t},s_{i,j,t}\}} \mathbb{E}_t \sum_{s=t}^{\infty} \left(\frac{1}{1+r^d}\right)^{s-t} \sum_{j=1}^{N} \Big(\underbrace{l_{i,j,t}\bar{R}_{i,j,t}y_{i,j,t}}_{\text{lending}} + \underbrace{l_{j,i,t}(r-r_{j,i,t})y_{j,i,t}}_{\text{borrowing}} - m_{i,j,t} - s_{i,j,t} \Big), \tag{7}$$

where the expected discounted payoff is expressed in terms of the expected surplus compared to the outside options provided by the central bank, and the maximization is subject to the restrictions imposed by the structure laid down in Sections 3.1–3.3. The interest rate r^d is used for discounting future cash flows; in our model, the interest rate banks can earn when depositing funds at the central bank. The intertemporal optimization problem is operationalized by conditioning on the bilateral equilibrium interest rates, $r_{i,j,t}$, characterized in Section 3.2. Hence, in this subsection these interest rates appear as a restriction on the optimization problem instead of one of the objective function's arguments.[15]

To solve the optimization problem using the calculus of variation, we impose appropriate smoothness conditions on the objective function and linearize part of the analytically intractable Euler equation for monitoring; see Appendix A for the details and derivations. We then obtain the optimal linearized bank-to-bank monitoring choice as the affine function,

$$m_{i,j,t} = a_m + b_m\tilde{\sigma}^2_{i,j,t} + c_m\mathbb{E}_t\tilde{\sigma}^2_{i,j,t+1} + d_m\mathbb{E}_tB_{i,j,t+1} + e_m\mathbb{E}_ty_{i,j,t+1}, \tag{8}$$

where the intercept and coefficients are functions of the structural parameters. The policy rule shows that bank i's optimal monitoring expenditures directed toward bank j depend on the current state of bank-to-bank credit-risk uncertainty, the expected future uncertainty, the expected volume of the loan, and on the expected probability of being contacted by bank j.[16]

We obtain an analytical solution for the optimal level of bank-to-bank search. The solution depends on bank j's expected surplus $\Delta_{i,j,t} := \mathbb{E}_t[y_{j,i,t}(r-r_{j,i,t})l_{j,i,t}]$ when borrowing from bank i:

$$s_{i,j,t} = \begin{cases} s(\Delta_{i,j,t}) & \text{for} \quad \Delta_{i,j,t}\lambda(s(\Delta_{i,j,t})) - s(\Delta_{i,j,t}) \geq 0 \\ 0 & \text{for} \quad \Delta_{i,j,t}\lambda(s(\Delta_{i,j,t})) - s(\Delta_{i,j,t}) < 0. \end{cases} \tag{9}$$

[14] The bargaining process fails if two banks are in contact but the bilateral equilibrium interest rate does not satisfy the participation constraints or if both banks are on the same side of the market, that is, both have positive or negative liquidity shocks.

[15] Note that actual default does not enter banks' objective functions ($\bar{R}_{i,j,t}y_{i,j,t}$ not $R_{i,j,t}y_{i,j,t}$) nor their constraint functions. What matters in the model is only the (perceived) probability of default that enters the pricing of interbank loans, as in Eq. (2). We do not incorporate actual bank default into the model because in the sample that we use for the parameter estimation, we do not observe any bank defaults. Moreover, actual bank default is not essential for understanding the basic mechanisms of peer monitoring, credit-risk uncertainty, and counterparty search that drive the observed market structure and its dynamics. Clearly, because there is no actual default event in the model, there is also no contagion through mutual credit exposure.

[16] Note that in our model we focus on bilateral interbank lending and the recourse to central bank facilities. Hence, the optimal monitoring decisions are based on interbank lending only, and do not reflect any other bilateral exposure between banks.

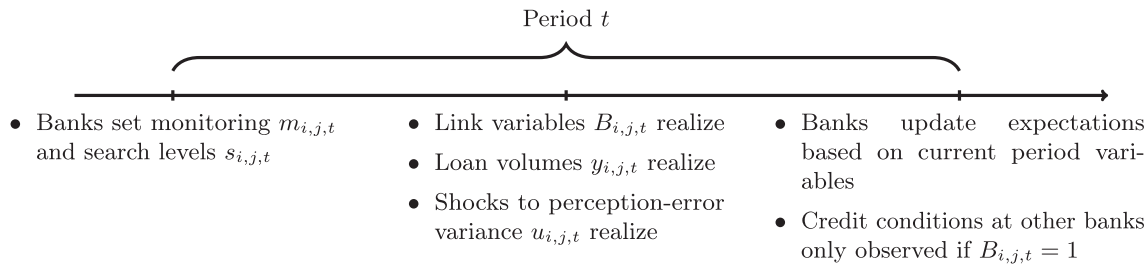

Fig. 1. Timeline Illustrating the Sequence of Events in Period t.

Here, the interior solution with positive search levels is obtained from the analytical solution to the first-order condition (see Appendix A) as

$$s(\Delta_{i,j,t}) := 1/\beta_\lambda \log\left(0.5\left(\sqrt{\Delta_{i,j,t}\beta_\lambda(\Delta_{i,j,t}\beta_\lambda - 4)} + \Delta_{i,j,t}\beta_\lambda - 2\right)e^{\alpha_\lambda\beta_\lambda}\right), \tag{10}$$

for $\Delta_{i,j,t}\beta_\lambda(\Delta_{i,j,t}\beta_\lambda - 4) \geq 0$. The optimal search strategy hence shows that for a positive expected return net of search cost, the solution satisfies Eq. (10), with $s(\cdot)' \geq 0$. Thus, search efforts increase in the expected surplus. Note that $\lambda(0) > 0$, so even without undertaking search efforts, two banks will eventually connect with each other and bargain about potential loan outcomes.

It is important to highlight that lender i's monitoring level with respect to borrower j depends on the expectation of being contacted for a loan. Similarly, borrower j's search effort with respect to lender i depends on the expected surplus that can be obtained from borrowing from bank i. This connection between monitoring and counterparty selection, linked by banks' profit expectations, generates an amplification mechanism that lies at the core of this model.

3.4.1. Adaptive expectations

The optimal monitoring and search levels in Eqs. (8) and (9) depend on expectations about bilateral credit availability and conditions. We assume that in the interbank market each bank forms bank-specific *adaptive expectations* about the credit conditions at other banks.[17] Following Chow (1989, 2011), the adaptive expectation of bank i concerning variable $x_{i,j,t}$, denoted by $x^*_{i,j,t} := \mathbb{E}_t x_{i,j,t+1}$, follows an exponentially weighted moving average (EWMA),

$$x^*_{i,j,t} = (1 - \lambda_x)x^*_{i,j,t-1} + \lambda_x x_{i,j,t}, \tag{11}$$

where all variables are in deviation from the mean steady-state values. Banks use this forecasting rule for variables that are always observed by bank i ($\tilde{\sigma}_{i,j,t+1}$ and $B_{i,j,t+1}$). The parameter $\lambda_x \in (0, 1)$ determines the weight of the new observations at time t relative to the previous expectation.

However, a crucial implication of the opaque OTC structure of the interbank market is that a bank learns about credit conditions (that is, volumes $y_{i,j,t+1}$ and rates $r_{i,j,t+1}$) at *other* banks only when contact is made (information about credit availability and conditions at other banks is not publicly available). Our model incorporates this feature of decentralized interbank markets by assuming that bank i uses the following forecasting rule,

$$x^*_{i,j,t} = (1 - \lambda_x)x^*_{i,j,t-1} + \lambda_x B_{i,j,t} x_{i,j,t}. \tag{12}$$

Recall that $B_{i,j,t}(s_{j,i,t}) = 1$ denotes an "open" connection. Hence, new information about a counterparty is added to the expectation only if the banks have established contact in period t; otherwise, the last forecast is not maintained but discounted by a factor $(1 - \lambda_x)$. Thus, if banks i and j are not in contact for many periods, their expectations converge to the mean steady-state values.

The formulation of the expectation mechanism completes the description of the model. Fig. 1 summarizes the sequence of events taking place within one period. From the structural model, we obtain a reduced form that allows simulations from the parametric model under some given parameter vector; details on the reduced-form representation and stability conditions are provided in Appendix B.

[17] The adoption of adaptive expectations is justified in the first place by the fact that in many settings, there exists very strong econometric evidence supporting the adaptive expectations hypothesis against the rational expectations hypothesis (see, for example, Chow, 1989; Chow, 2011). Specifically, Evans and Honkapohja (2001) show that in many ways adaptive expectations are the most rational forecasting method to use when the true data-generating process is unknown. This argument seems especially relevant for modeling decisions in a highly complex system such as an OTC trading network. Second, adaptive expectations are much easier to handle. Indeed, it is impossible to use the model's deterministic steady-state as an approximation point for perturbation methods (see Appendix A). This renders the rational expectations solution computationally impractical. On the contrary, since adaptive expectations are solely dependent on past observations, the numerical nature of the equilibrium point does not present extra difficulties.

4. Parameter estimation

We now turn to the estimation of the structural model's parameters using loan-level data from the Dutch overnight interbank lending market. To estimate the parameters of the complex dynamic network model (nonlinearity and nonstandard distributions), we propose a simulation-based indirect inference estimator that builds on an appropriate set of auxiliary statistics.

4.1. Indirect inference network estimator

Following the principle of indirect inference introduced in Gourieroux et al. (1993), we estimate the vector of parameters $\boldsymbol{\theta}_T$ by minimizing the quadratic distance between the auxiliary statistics $\hat{\boldsymbol{\beta}}_T$ obtained from the observed data $X_1, \ldots, X_T$, and the average of the auxiliary statistics $\tilde{\boldsymbol{\beta}}_{TS}(\boldsymbol{\theta}) := (1/S)\sum_{s=1}^{S}\tilde{\boldsymbol{\beta}}_{T,s}(\boldsymbol{\theta})$ obtained from S simulated datasets $\{\tilde{X}_{1,s}(\boldsymbol{\theta}), \ldots, \tilde{X}_{T,s}(\boldsymbol{\theta})\}_{s=1}^{S}$ generated under $\boldsymbol{\theta} \in \Theta$. Formally, the indirect inference estimator is thus given as

$$\hat{\boldsymbol{\theta}}_T := \arg\max_{\boldsymbol{\theta}\in\Theta}\left[\hat{\boldsymbol{\beta}}_T - \frac{1}{S}\sum_{s=1}^{S}\tilde{\boldsymbol{\beta}}_{T,s}(\boldsymbol{\theta})\right]' \mathbf{W}_T \left[\hat{\boldsymbol{\beta}}_T - \frac{1}{S}\sum_{s=1}^{S}\tilde{\boldsymbol{\beta}}_{T,s}(\boldsymbol{\theta})\right],$$

where Θ denotes the parameter space of $\boldsymbol{\theta}$ and $\mathbf{W}_T$ is a weight matrix. Under appropriate regularity conditions, this estimator is consistent and asymptotically normal. In particular, consistency holds as long as, for given $S \in \mathbb{N}$, the auxiliary statistics converge in probability to singleton limits $\tilde{\boldsymbol{\beta}}_{T,s} \xrightarrow{p} \boldsymbol{\beta}(\boldsymbol{\theta})\ \forall\boldsymbol{\theta}$ and $\hat{\boldsymbol{\beta}}_T \xrightarrow{p} \boldsymbol{\beta}(\boldsymbol{\theta}_0)$ as $T \to \infty$, where $\boldsymbol{\theta}_0$ denotes the model parametrization that has generated the data, while the so-called *binding function* $\boldsymbol{\beta} : \Theta \to \mathcal{B}$ that maps the structural parameters into the auxiliary statistics is injective. Convergence in probability is precisely ensured through the application of the law of large numbers for strictly stationary and ergodic data (see White, 2001). Similarly, asymptotic normality of the estimator is obtained if the auxiliary statistics $\hat{\boldsymbol{\beta}}_T$ and $\tilde{\boldsymbol{\beta}}_{T,s}$ are asymptotically normal (see Gourieroux et al., 1993). By application of a central limit theorem (see, for example, White, 2001), the asymptotic normality of the auxiliary statistics can again be obtained by appealing to the strict stationarity and ergodicity of both the observed and simulated data.

The injective nature of the binding function is the fundamental identification condition which ensures that the structural parameters are appropriately described by the auxiliary statistics. This condition cannot be verified algebraically since the binding function is analytically intractable. However, identification will be ensured as long as the set of auxiliary statistics adequately describes both observed and simulated data. Hence, we select auxiliary statistics that provide a comprehensive characterization of the interbank market represented by the network of bilateral loans and the associated loan volumes and interest rates. Specifically, in line with the estimation of dynamic models (see, for example, DeJong and Dave, 2006; Ruge-Murcia, 2007), we use the auto-covariance structure as well as higher-order moments, such as measures of skewness and kurtosis that are justified by the model's nonlinearity.

In addition to these standard auxiliary statistics, we base the indirect inference estimator on auxiliary statistics that specifically characterize the topological structure of the interbank lending network. In particular, since our model focuses on explaining the economic mechanisms behind the observed patterns of relationship lending and the sparse core-periphery structure, we include statistics that measure these characteristics. Therefore, we follow the large empirical literature on the structure of interbank lending networks and use key network statistics that are common in empirical analysis (see, for example, Bech and Atalay, 2010; Jackson, 2008). Moreover, we only include network statistics that are easy to compute, due to the large number of simulated networks in the estimation procedure.

First, we consider global network statistics. In particular, the *density*, defined as the ratio of the actual to the potential number of links, is a standard measure of a network's connectivity. A low density characterizes a sparse network with few links. *Reciprocity* measures the fraction of reciprocal links in a directed network. For the interbank market, this relates to the degree of mutual lending between banks. The *stability* of a sequence of networks refers to the fraction of links that do not change between two adjacent periods. Note that all three statistics are bounded between zero and one.

Second, we include bank-level (node-level) network statistics. The (unweighted) *in-degree* of a bank is defined as the number of lenders it is borrowing from, and the (unweighted) *out-degree* as the number of borrowers to which it is lending. We summarize this bank-level information using the mean and standard deviation of the (in-/out-) degree distribution as well as its skewness. The (local) *clustering coefficient* of a node quantifies how close its neighbors are to being a clique (complete graph). In the interbank network, this coefficient measures how many of a bank's counterparties have mutual credit exposures. We compute the clustering coefficients for directed networks as proposed by Fagiolo (2007) and consider the average clustering coefficient as an auxiliary statistic.

Third, we focus on simple bilateral network statistics that measure the intensity of a bilateral trading relationship based on past lending activity during a rolling window. Similar to Furfine (1999) and Cocco et al. (2009), we compute the number of loans bank i granted to bank j during the previous week and denote this variable by $l^{rw}_{i,j,t}$. We then compute a cross-sectional correlation between these relationship variables and loan outcomes at time t (the decision to grant a loan and interest rate). The first variable $\mathrm{Corr}(l_{i,j,t}, l^{rw}_{i,j,t-1})$ is a measure of the bilateral stability of lending relations, while $\mathrm{Corr}(r_{i,j,t}, l^{rw}_{i,j,t-1})$ is a proxy for the effects of relationship lending on interest rates.

Table 1
Finite-sample distribution of network estimator under correct specification.

	θ_0	mean($\hat{\theta}$)	p10($\hat{\theta}$)	p50($\hat{\theta}$)	p90($\hat{\theta}$)	RMSE($\hat{\theta}$)	MAE($\hat{\theta}$)
$\beta_{\phi,1}$	9.6000	9.6604	9.0842	9.6322	10.1781	0.5941	0.3646
$\beta_{\phi,2}$	1.0000E-4	1.0060E-4	9.5910E-5	1.0073E-4	1.0546E-4	9.5491E-6	4.4641E-6
α_σ	1.2890	1.2961	1.2305	1.2943	1.3858	0.0692	0.0472
γ_σ	0.6648	0.6653	0.6348	0.6662	0.6934	0.0255	0.0173
δ_σ	0.3383	0.3423	0.3127	0.3401	0.3694	0.0277	0.0175
α_λ	1.0000E-4	1.0031E-4	9.5010E-5	1.0057E-4	1.0723E-4	9.6832E-6	4.6303E-6
β_λ	72.8331	74.1304	70.0855	73.1026	80.4376	4.8176	2.9613
σ^*_μ	1.9903	2.0235	1.7749	2.0253	2.2246	0.2285	0.1478
μ_σ	1.9492	1.8493	1.6130	1.8754	2.0524	0.2154	0.1525
σ_σ	1.9810	1.9741	1.7028	1.9693	2.2113	0.2178	0.1499
ρ_ζ	0.7826	0.7927	0.6955	0.7915	0.8810	0.0842	0.0586
λ_B	0.9278	0.9209	0.8618	0.9281	0.9810	0.0638	0.0411
λ_y	0.8472	0.8677	0.7468	0.8846	0.9783	0.0871	0.0723
λ_r	0.4008	0.4095	0.3873	0.4080	0.4324	0.0363	0.0207
$\lambda_{\bar{\sigma}}$	0.0318	0.0320	0.0303	0.0320	0.0334	0.0017	0.0010
θ	0.6896	0.6786	0.6257	0.6849	0.7274	0.0520	0.0330

Notes: The table reports key statistics of the finite-sample distribution for the indirect inference network estimator. Results are based on a Monte Carlo study with 250 repetitions, where the data are generated under the parametrization estimated from the Dutch interbank network data with $N = 50$ and $T = 1000$, and $S = 24$ network paths. RMSE is the root mean squared error. Calibrated parameters are similar to Table 3.

We compute all the described network statistics for each lending network within the sequence of networks such that we obtain a sequence of network statistics associated with the sequence of networks. We then obtain the unconditional means, variance, and/or autocorrelation of these sequences as auxiliary statistics and base the parameter estimations only on the values of the auxiliary statistics. In Appendix C, we provide the formulae of the described network statistics.

Our estimator is based on a quadratic objective function with a diagonal weight matrix $\mathbf{W}_T$, as we refrain from using an asymptotically efficient weight matrix. This is because the inverse of the covariance matrix is only optimal under an axiom of correct specification. In addition, even under the correct specification, the (asymptotically) optimal weight matrix can lead to a larger variance of the estimator in finite samples. Moreover, for theoretical economic reasons, there are a number of auxiliary statistics that we wish to approximate better than others. As such, we adopt a matrix $\mathbf{W}_T$ corresponding to an identity matrix, but the weight of the average degree (scaled density) and Corr($l_{i,j,t}, l^{rw}_{i,j,t-1}$) are set to 10 and the weight of Corr($r_{i,j,t}, l^{rw}_{i,j,t-1}$) is set to 50 because we want to match these characteristics particularly well, given our focus on trading relationships. However, our results are qualitatively similar if we use an identity matrix as the weight matrix.[18]

As mentioned above, an injective mapping between the auxiliary statistics and structural parameters is the crucial identification condition of the indirect inference estimator. However, this condition cannot be verified algebraically since the binding function is analytically intractable. Therefore, we next conduct an simulation study to assess the sensitivity of the auxiliary statistics. In particular, we vary the structural parameters and analyze how the network structure responds as characterized by key auxiliary statistics. Fig. 2 shows how the mean density, reciprocity, skewness of out-degree and in-degree distribution, mean monitoring and mean search respond to changes in structural parameters by $\pm 10\%$ from the values $\hat{\boldsymbol{\theta}}_T$ that we estimate in our empirical application (see Section 4.3). Specifically, we focus on varying the coefficient of monitoring ($\beta_{\phi,1}$) in Eq. (3), the autoregressive coefficient of the log perception-error variance (γ_σ) in Eq. (1) and the parameter that determines the location of the logistic link probability function (α_λ), while holding constant all other parameters at the estimated values. Overall, the analysis reveals that the auxiliary statistics are (at least locally) sensitive to changes in key structural model parameters (results for other paramers are similar and can be obtained from the authors). Hence, the simulation study supports the notion that the necessary condition (sensitivity of auxiliary statistics) for the identification of the indirect inference estimator is met. Additional discussion of the sensitivity analysis can be found in the Appendix D.

The sensitivity analysis reported above, describing how the auxiliary statistics $\tilde{\boldsymbol{\beta}}_{T,S}(\boldsymbol{\theta})$ are affected by changes in the auxiliary parameters $\boldsymbol{\theta}$, gives us confidence that the binding function is injective and $\boldsymbol{\theta}_0$ is well identified. To further strengthen the evidence on the econometric validity of our analysis, we next evaluate the finite-sample properties of the indirect inference network estimator using a Monte Carlo study. In particular, the simulated data in the MC study are generated under

[18] In all the estimations, we use for computational reasons $S = 24$ simulated network paths, each with a length of 4000 periods, with the initial 1000 periods burned to minimize dependence on the initial values (the effective sample size is 3000 periods). In the estimation, some of the structural parameters are calibrated as these are not identified by the data. For example, it is clear that several combinations of β_σ, $\beta_{1,\phi}$, and $\beta_{2,\phi}$ imply the same distribution for the data, and hence, also for the auxiliary statistics. The same implication applies for ϵ and σ. Further, we fix the common default threshold ϵ and the common true variance of the financial distress σ^2 to obtain an upper bound on the true probability of default of 0.01. We calibrate the corridor width to the average value of 1.5 percentage points observed in our sample period and set the discount rate to 1.75% per annum. The scaling parameter of the logistic function that approximates the step function when solving the model is set to 200.

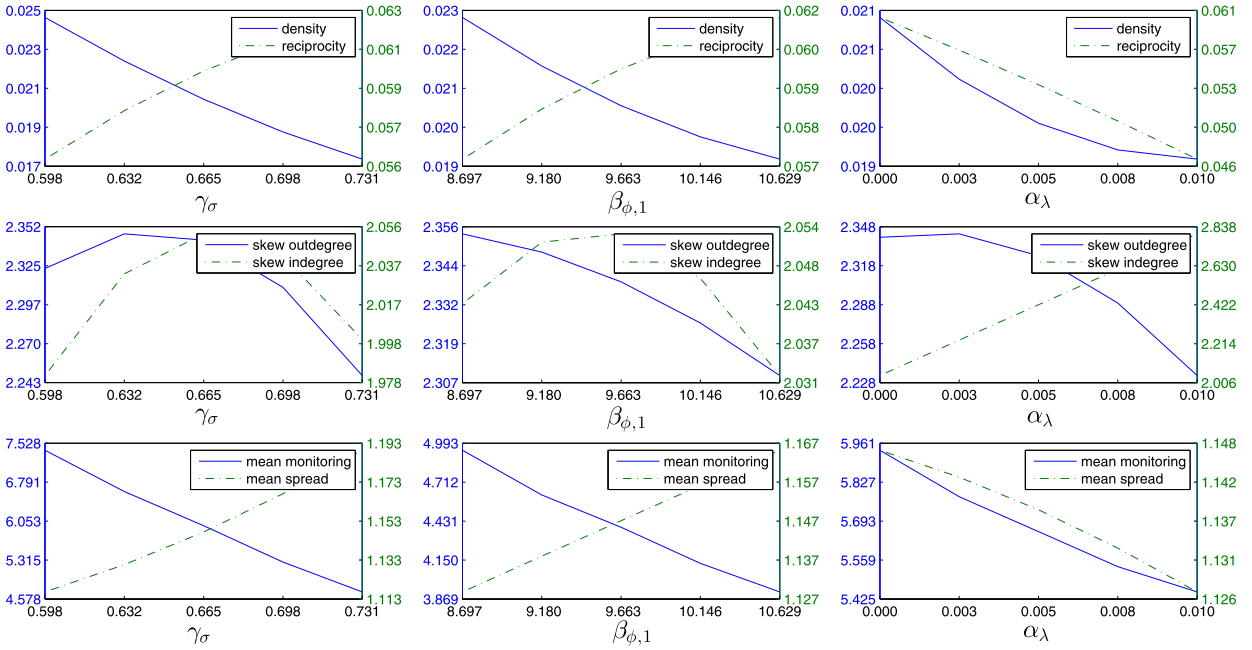

Fig. 2. Sensitivity analysis of auxiliary statistics. *Notes:* Simulated mean of network statistics as a function of key structural parameters related to credit-risk uncertainty (γ_σ), efficacy of peer monitoring ($\beta_{\phi,1}$), and search frictions (α_λ). Parameters range from $\pm 10\%$ around estimated values, holding fixed all other parameters. Each figure is based on 5000 MC repetitions, each with $T = 500$. Left (right) axes correspond to solid (dashed) lines. Source: Authors' calculations.

the parameter vector that we estimate from the observed Dutch interbank network (see Section 4.3, Table 2). Given the large computational burden of the exercise, we focus on 250 MC repetitions and a network of size $N = 50$, similar to our empirical application. Table 1 presents key statistics of the finite sample distribution under correct specification. The MC results show that the estimator is closely centered around the true parameter used to simulate the data, both in terms of mean and median of the finite-sample distribution. For example, the mean and median of the parameter estimate of $\beta_{\phi,1}$ that governs the effectiveness of monitoring on reducing the perception error variance is close to the true value. Moreover, the root mean squared error (RMSE) relative to the true parameter value is small with 6% (=0.5941/9.6601). On the other hand, other parameters exhibits somewhat larger RMSEs. For example, the parameter estimates that govern the liquidity shock distribution have a wider dispersion with relative RMSE between 8% and 11%. In Appendix D, we discuss futher MC results of the small-sample behavior of the estimator under incorrect specification.

The sensitivity analysis in combination with the Monte Carlo study of the finite-sample distribution suggest that the estimator does not suffer from identification problems. In any case, given the complexity of the structural model, we also

Table 2
Descriptive statistics.

Statistic	Mean	Std	Autocorr
Density	0.0212	0.0068	0.8174
Reciprocity	0.0819	0.0495	0.2573
Stability	0.9818	0.0065	0.8309
Mean out-/in-degree	1.0380	0.3323	0.8174
Mean clustering	0.0308	0.0225	0.4149
Corr($r_{i,j,t}, l^{rw}_{i,j,t-1}$)	−0.0716	0.1573	0.4066
Corr($l_{i,j,t}, l^{rw}_{i,j,t-1}$)	0.6439	0.0755	0.4287
Mean log volume	4.1173	0.2818	0.4926
Mean spread	0.2860	0.3741	0.9655

Notes: The table reports moment statistics for different sequences of network statistics and cross-sectional correlations that characterize the sequence of observed Dutch unsecured interbank lending networks. The statistics are computed on a sample of daily frequency from February 18, 2008, to April 28, 2011.

allow for the possibility of some form of identification failure. In particular, following Blasques and Duplinskiy (2018), we note that a penalized indirect inference estimator can be used to ensure identification of the parameter vector.

The penalized indirect inference estimator is defined as

$$\hat{\boldsymbol{\theta}}_T^p := \arg\max_{\boldsymbol{\theta}\in\Theta} \left[\hat{\boldsymbol{\beta}}_T - \frac{1}{S}\sum_{s=1}^{S}\tilde{\boldsymbol{\beta}}_{T,s}(\boldsymbol{\theta})\right]' \mathbf{W}_T \left[\hat{\boldsymbol{\beta}}_T - \frac{1}{S}\sum_{s=1}^{S}\tilde{\boldsymbol{\beta}}_{T,s}(\boldsymbol{\theta})\right] + \pi_T(\boldsymbol{\theta}),$$

where $\pi_T\colon \Theta \to [0, \infty)$ is a penalty function that plays a role similar to that of a prior in Bayesian estimation. Lemma 1 below states the conditions for consistency of the penalized indirect inference estimator. The highlight of this lemma is the fact that it does not require the usual strong identification condition that the binding $\boldsymbol{\beta}(\boldsymbol{\theta})$ be injective. Instead, it requires only that $\boldsymbol{\theta}_0$ be identified with respect to the penalized criterion function which is partially shaped by the penalty function π_T; see Blasques and Duplinskiy (2018) for the proof and additional details.

Lemma 1. *(Consistency) Let Θ be compact and $\hat{\boldsymbol{\beta}}_T \xrightarrow{as} \boldsymbol{\beta}(\boldsymbol{\theta}_0)$ and $\tilde{\boldsymbol{\beta}}_{T,s}(\boldsymbol{\theta}) \xrightarrow{as} \boldsymbol{\beta}(\boldsymbol{\theta})$ converges uniformly in $\boldsymbol{\theta}$. Let the penalty function $\pi_T(\boldsymbol{\theta}) \xrightarrow{as} \pi(\boldsymbol{\theta})$ converge uniformly in $\boldsymbol{\theta}$ to some limit penalty function $\pi\colon \Theta \to [0, \infty)$. Finally, suppose that there exists a unique point $\boldsymbol{\theta}_0 \in \Theta$ that minimizes the limit penalized criterion. Then $\hat{\boldsymbol{\theta}}_T \xrightarrow{as} \boldsymbol{\theta}_0$ as $T \to \infty$.*

Lemma 2 below further shows that statistical inference is possible in a weak identification setting. Following Stock and Wright (2000), we let the structural parameter vector $\boldsymbol{\theta}$ be split as follows $\boldsymbol{\theta} = (\boldsymbol{\theta}^{1'}, \boldsymbol{\theta}^{2'})'$ where $\boldsymbol{\theta}^1$ is a sub-vector that is well identified, and $\boldsymbol{\theta}^2$ is a sub-vector that is weakly identified in the sense that the II criterion is asymptotically flat in $\boldsymbol{\theta}^2$. Specifically, let the binding function be given by $\boldsymbol{\beta}_T(\boldsymbol{\theta}_0) - \boldsymbol{\beta}_T(\boldsymbol{\theta}) = m_1(\boldsymbol{\theta}^1) + m_{2,T}(\boldsymbol{\theta})/r_T$ where *(i)* m_1 is continuous in $\boldsymbol{\theta}^1$ and $m_1(\boldsymbol{\theta}^1) = 0$, $m_1(\boldsymbol{\theta}^1) \neq 0 \ \forall\ \boldsymbol{\theta}^1 \neq \boldsymbol{\theta}_0^1$; *(ii)* $m_{2,T}$ is continuous on Θ and $\sup_{\boldsymbol{\theta}\in\Theta} |m_{2,T}(\boldsymbol{\theta}) - m_2(\boldsymbol{\theta})| \to 0$ a.s. as $T \to \infty$; and *(iii)* $r_T \to \infty$ as $T \to \infty$.[19]

For simplicity, Lemma 2 focuses on the case of a well centered penalty function satisfying $\nabla_1 \pi_T(\boldsymbol{\theta}_0) = \mathbf{0}$ and $\nabla_2 \pi_T(\boldsymbol{\theta}_0) = \mathbf{0}$; where $\nabla_{ij}^n \pi$ denotes the (i, j)-subset of the n-th derivative of the limit penalty function π. For this class of penalties, Lemma 2 shows that, *(i)* if the penalty function imposes no cross-restrictions, i.e. if $\nabla_{12}^2 \pi(\boldsymbol{\theta}_0) = \mathbf{0}$ and $\nabla_{21}^2 \pi(\boldsymbol{\theta}_0) = \mathbf{0}$, then inference is possible on the strongly identified sub-vector $\boldsymbol{\theta}^1$; and *(ii)* if the penalty function imposes cross-restrictions, i.e. if $\nabla_{12}^2 \pi(\boldsymbol{\theta}_0) \neq \mathbf{0}$, $\nabla_{21}^2 \pi(\boldsymbol{\theta}_0) \neq \mathbf{0}$, then inference is possible on the entire vector $\boldsymbol{\theta}$; see Blasques and Duplinskiy (2018) for the proof and for the exact form of the asymptotic covariance matrices $\mathbf{W}^1$ and $\mathbf{W}$.

Lemma 2. *(Asymptotic normality) Suppose the penalty is well centered $\nabla_1 \pi_T(\boldsymbol{\theta}_0) = \mathbf{0}$ and $\nabla_2 \pi_T(\boldsymbol{\theta}_0) = \mathbf{0}$ for every $T \in \mathbb{N}$. If $\nabla_{12}^2 \pi(\boldsymbol{\theta}_0) = \mathbf{0}$, $\nabla_{21}^2 \pi(\boldsymbol{\theta}_0) = \mathbf{0}$, then $\hat{\boldsymbol{\theta}}_{T,S}^2 \xrightarrow{a.s.} \boldsymbol{\theta}_0^2$ and $\sqrt{T}(\hat{\boldsymbol{\theta}}_{T,S}^1 - \boldsymbol{\theta}_0^1) \xrightarrow{d} N(\mathbf{0}, \mathbf{W}^1)$ as $T \to \infty$. If $\nabla_{12}^2 \pi(\boldsymbol{\theta}_0) \neq \mathbf{0}$, $\nabla_{21}^2 \pi(\boldsymbol{\theta}_0) \neq \mathbf{0}$, then $\sqrt{T}(\hat{\boldsymbol{\theta}}_{T,S} - \boldsymbol{\theta}_0) \xrightarrow{d} N(\mathbf{0}, \mathbf{W})$ as $T \to \infty$.*

In practice, we found that for our dynamic interbank network model, the difference in the point estimates obtained with and without a penalty function were negligible when the penalty function is weak.

4.2. Data description

The original raw data that we use in the estimation procedure comprise the daily bilateral lending volumes and interest rates realized in the overnight unsecured lending market among all Dutch banks. In particular, our empirical analysis is based on a confidential transaction-level dataset of interbank loans compiled by central bank authorities, based on payment records in the European large-value payment system TARGET2. This panel of Dutch interbank loans has been inferred by using a modified and improved version of the algorithm proposed by Furfine (1999) for the U.S. Fedwire system; for details on the dataset and methodology, see Heijmans et al. (2011) and Arciero et al. (2013).

Our interbank loan-level dataset contains observations on daily bilateral volumes ($y_{i,j,t}$) and interest spreads ($r_{i,j,t}$) for the sample from February 19, 2008, through April 28, 2011 ($T = 810$ trading days). From these data, we construct the loan indicator $l_{i,j,t}$ that equals one if a loan from lender i to borrower j at day t is observed, and is zero otherwise. For computational reasons, we focus on overnight interbank lending among the 50 largest Dutch banks based on the frequency of their overnight trading (as both borrower and lender) throughout the entire sample period (banks are consolidated at the bank holding company level). As a result, the data from which the auxiliary statistics are obtained consist of three $50 \times 50 \times 810$ arrays with elements $l_{i,j,t}$, $y_{i,j,t}$, and $r_{i,j,t}$. The arrays for $y_{i,j,t}$ and $r_{i,j,t}$ contain missing values if and only if $l_{i,j,t} = 0$.[20]

Table 2 shows the key summary statistics of the data used in the analysis. Note that: (i) the moments of bilateral volumes of granted loans are for values stated in (logarithm of) EUR millions; (ii) the moments of bilateral interest rates of granted loans are reported in percentage points per annum above the ECB deposit facility rate (the interest rate corridor's

[19] As noted in Stock and Wright (2000), this type of weak identification corresponds to the specification of a *drifting DGP*, in the terminology of Davidson and MacKinnon (1993).

[20] The dataset contains only loans of at least 1 million euros in volume, as typically banks with liquidity shocks below that amount do not go to the interbank market. Therefore, Eq. (5) for the volumes of granted loans changes accordingly to $y_{i,j,t} = \min\{\zeta_{i,j,t}^i, -\zeta_{i,j,t}^j\}\mathbb{I}(\zeta_{i,j,t}^i \geq c)\mathbb{I}(\zeta_{i,j,t}^j \leq c)$, with $c = 1$ EUR millions.

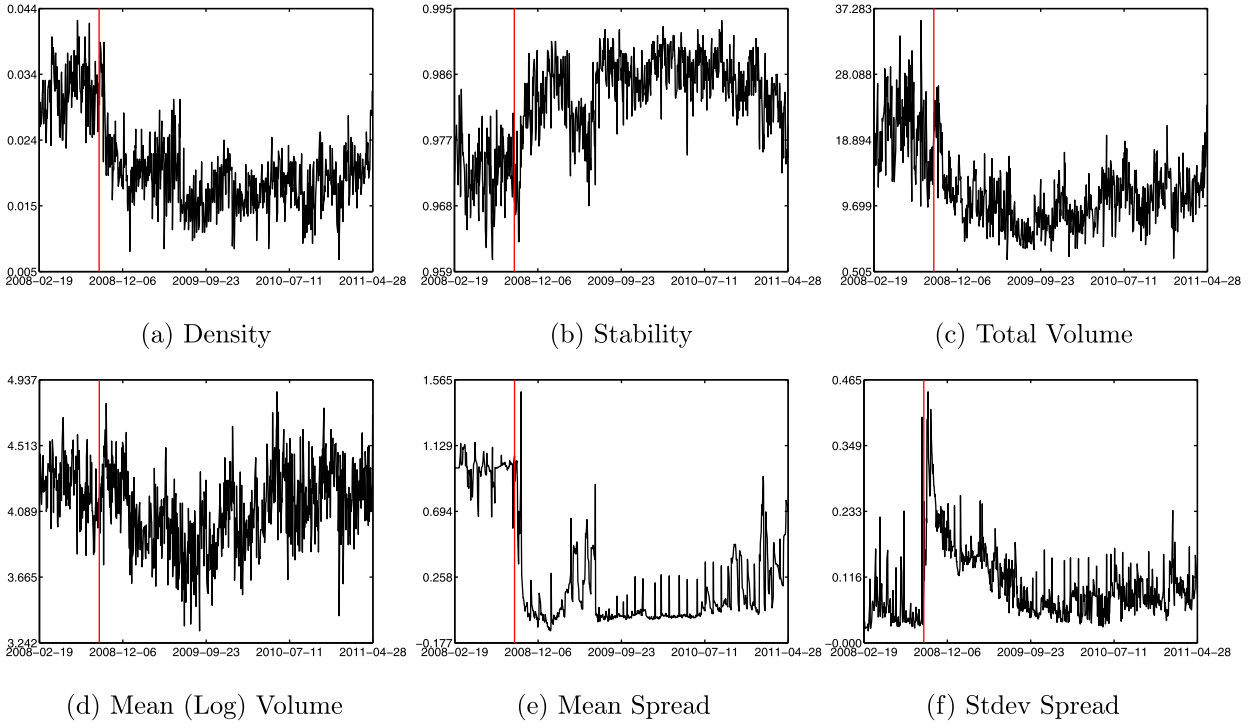

Fig. 3. Daily network time series plots: February 18, 2008, to April 28, 2011. (For interpretation of the references to color in this figure legend, the reader is referred to the web version of this article.) *Notes:* Time series plots of daily network density, stability, total traded volume (in EUR billions), and mean loan volume (in log EUR millions), mean spread (to deposit rate), and standard deviation of granted loans from February 18, 2008, to April 28, 2011. Vertical red line corresponds to Lehman's failure on September 15, 2008. *Source:* Authors' calculations.

lower bound); (iii) the daily interbank network is very sparse, with a mean density of 0.02 (on average, 1.04 lenders and borrowers) and low clustering; (iv) the distribution of interest rates, volumes, degree centrality, and clustering are highly skewed. It is also important to emphasize that the high autocorrelation of the density, the high stability of the network, and the positive expected correlation between current period lending and past lending activity can be seen as evidence of "trust" relations between banks, thus showing that past trades affect future trading opportunities. Similarly, the negative expected correlation between past lending activity and current interest rates provides evidence of lower perceived default risk that may result from monitoring efforts postulated by the proposed structural model.

Fig. 3 presents the evolution of the daily network density, stability, average (log) volume, total volume, and the mean and standard deviation of the daily spreads over time during the sample period. From the plots, we see that the network density and total trading volume declined after Lehman's failure on September 15, 2008 (indicated by the vertical red line). In economic terms, the total trading volume declines from about EUR 20 billion to EUR 10 billion. At the same time, the network stability and the daily cross-sectional standard deviation of interest rate spreads more than tripled. Moreover, the mean interest rate spreads of granted loans are close to the deposit facility as of October 2008, when the ECB introduced its fixed-rate full allotment policy. Further, the plots reveal that the data exhibit well documented end-of-maintenance period effects that we clean out in the construction of the auxiliary statistics by regressing each sequence of network statistics on end-of-maintenance period dummies before computing auxiliary statistics.

4.3. Estimation results

We now turn to the estimation results for the interbank network model. Table 3 shows the point estimates $\hat{\boldsymbol{\theta}}_T$ and standard errors of the structural parameters using the auxiliary statistics reported in Table 5. Naturally, standard errors are not provided for calibrated parameters. For comparison with the indirect inference estimates, we also present $\boldsymbol{\theta}^r$, an alternative calibrated parameter vector, which equals $\hat{\boldsymbol{\theta}}_T$ but restricts the effects of monitoring to zero ($\beta_{\phi,1} = 0$). By changing only one parameter of $\hat{\boldsymbol{\theta}}_T$, we analyze the role of peer monitoring with a *ceteris paribus* argument. Table 3 also depicts the estimated parameter vector $\hat{\boldsymbol{\theta}}_T^r$ of the restricted model ($\beta_{\phi,1} = 0$) to analyze the fit of the model without monitoring when the other parameters are re-estimated and fully determined by the data.

Table 3
Estimated structural parameter values.

		Calibrated	Estimated		Estimated	
		without monitoring	without monitoring		withMonitoring	
Structural parameter		$\boldsymbol{\theta}^r$	$\hat{\boldsymbol{\theta}}_T^r$	ste($\hat{\boldsymbol{\theta}}_T^r$)	$\hat{\boldsymbol{\theta}}_T$	ste($\hat{\boldsymbol{\theta}}_T$)
Added information	α_ϕ	−1.5000	−1.5000	–	−1.5000	–
	$\beta_{\phi,1}$	0.0000	0.0000	–	9.6631	0.0006
	$\beta_{\phi,2}$	0.0001	0.1386	0.0069	0.0001	0.0445
Perception error variance	α_σ	1.2890	1.2449	0.0151	1.2890	0.0028
	β_σ	−2.0000	−2.0000	–	−2.0000	–
	γ_σ	0.6648	0.6351	0.0063	0.6648	0.0183
	δ_σ	0.3383	1.7214	0.0069	0.3383	0.0451
Search technology	α_λ	0.0001	0.0208	0.0566	0.0001	0.1159
	β_λ	72.833	102.82	0.0009	72.833	0.0006
Liquidity shocks	μ_μ	0.0000	0.0000	–	0.0000	–
	σ_μ^*	1.9903	3.6563	0.0024	1.9903	0.0228
	μ_σ	1.9492	0.6120	0.0033	1.9492	0.0218
	σ_σ	1.9810	4.5002	0.0051	1.9810	0.0213
	ρ_ζ	−0.7826	−0.0170	0.0064	−0.7826	0.0423
Expectations	λ^y	0.8472	0.8809	0.0226	0.8472	0.0443
	λ^B	–	–	–	0.9278	0.0470
	λ^r	0.4008	0.0180	0.0271	0.4008	0.0466
	$\lambda^{\tilde{\sigma}}$	–	–	–	0.0318	0.0414
Bargaining power lender	θ	0.6897	0.0054	0.0226	0.6896	0.0441
Interest rate corridor width	r	1.5000	1.5000	–	1.5000	–
Default threshold	ϵ	3.0000	3.0000	–	3.0000	–
Financial distress std.	σ	0.1000	0.1000	–	0.1000	–
Discount rate	r^d	1.7500	1.7500	–	1.7500	–

Notes: This table reports the estimated structural parameters of the unrestricted model $\hat{\boldsymbol{\theta}}_T$ and corresponding standard errors. For comparison, this table also reports the estimated parameter $\hat{\boldsymbol{\theta}}_T^r$ of the restricted model without monitoring ($\beta_{\phi,1}$=0), as well as the calibrated parameter $\boldsymbol{\theta}_a$ that equals $\hat{\boldsymbol{\theta}}_T$ but sets the effect of monitoring to zero ($\beta_{\phi,1}$=0). For calibrated parameters (details see footnote 18), no standard errors are reported. The indirect inference estimator is based on $S = 24$ simulated network paths, each of length 3000 periods, and the auxiliary statistics reported in Table 5. The parameters λ^B and $\lambda^{\tilde{\sigma}}$ are not part of the restricted model without monitoring. Note also that $\sigma_\mu^* = \log(\sigma_\mu)$.

Table 4
Coefficients of the linear policy rule for optimal monitoring as implied by $\hat{\boldsymbol{\theta}}_T$.

Variable	$\tilde{\sigma}_{i,j,t}$	$\mathbb{E}_t\tilde{\sigma}_{i,j,t+1}$	$\mathbb{E}_t B_{i,j,t+1}$	$\mathbb{E}_t y_{i,j,t+1}$
Coefficient	0.0024	−0.0043	0.0348	0.0019

The parameter estimates $\hat{\boldsymbol{\theta}}_T$ reported in Table 3 are interesting in several respects. First, the autoregressive log-variance process's relatively large and significant intercept can be seen as evidence for high levels of prevailing bank-to-bank uncertainty. Also, the autoregressive parameter γ_σ is estimated to be 0.66, indicating that in the absence of new information, there is a positive autocorrelation in bilateral credit-risk uncertainty. The estimate of the scaling parameter δ_σ is positive and significant, indicating that shocks to credit-risk uncertainty are important drivers of bank-to-bank uncertainty. Moreover, $\beta_{\phi,1}$, the estimated coefficient that determines the effect that peer monitoring has on the additional information about credit risk, is positive and statistically significant. Hence, we find evidence that monitoring is a significant factor in reducing the prevailing bank-to-bank uncertainty regarding counterparty risk.[21] On the other hand, the estimated coefficient that determines a transaction's effect is close to zero and statistically insignificant. This result suggests that credit-risk uncertainty is not mitigated by repeated transactions, but depends on monitoring efforts.[22]

Second, the positive estimates for α_λ and β_λ show that counterparty search is a crucial feature in the formation of interbank networks. In particular, the large and significant estimate for β_λ is 73, which suggests that links are not randomly formed, but rather are strongly influenced by banks' search for preferred counterparties. With such large scaling, the logistic function mimics a step function quite well. The significant role of endogenous counterparty selection also highlights

[21] Additional estimations for subsamples, presented in Appendix Table 3, show that after Lehman's failure the effect of monitoring is quantitatively stronger. Overall, the qualitative model implications, however, remain robust to estiamtes based on subsamples, and we focus the remaining discussion on the model estimated from the full data.

[22] The restricted model's estimation results show that without monitoring, the effects of past transactions on the reduction of bank-to-bank uncertainty is stronger. Hence, the restricted model attributes part of the effects of monitoring to the mere existence of past trading activity.

Table 5
Auxiliary network statistics.

	Simulated values			Observed values	
Auxiliary statistic	Calibrated without monitoring $\tilde{\boldsymbol{\beta}}_{TS}(\boldsymbol{\theta}^r)$	Estimated without monitoring $\tilde{\boldsymbol{\beta}}_{TS}(\tilde{\boldsymbol{\theta}}^r_T)$	Estimated with monitoring $\tilde{\boldsymbol{\beta}}_{TS}(\tilde{\boldsymbol{\theta}}_T)$	$\hat{\boldsymbol{\beta}}_T$	ste($\hat{\boldsymbol{\beta}}_T$)
Density (Mean)	0.1121	0.0201	0.0193	0.0212	0.0026
Reciprocity (Mean)	0.0453	0.0005	0.0627	0.0819	0.0029
Stability (Mean)	0.8247	0.9837	0.9795	0.9818	0.0025
Avg clustering (Mean)	0.1097	0.0042	0.0347	0.0308	0.0027
Avg degree (Mean)	5.4948	0.9870	0.9441	1.0380	0.1291
Std outdegree (Mean)	3.2901	1.3501	1.6547	1.8406	0.0918
Skew out-degree (Mean)	0.4512	1.3604	2.3649	2.8821	0.3537
Std in-degree (Mean)	4.7450	1.3833	1.6950	1.6001	0.0995
Skew in-degree (Mean)	0.3300	1.3971	2.2801	2.4030	0.3143
Corr($r_{i,j,t}, l^{rw}_{i,j,t-1}$) (Mean)	0.0000	−0.1578	−0.1231	−0.0716	0.0113
Corr($l_{i,j,t}, l^{rw}_{i,j,t-1}$) (Mean)	0.2345	0.4259	0.6001	0.6439	0.0107
Avg log volume (Mean)	2.8298	4.1064	3.9422	4.1173	0.0516
Std log volume (Mean)	1.0547	1.0196	1.0865	1.6896	0.0200
Skew log volume (Mean)	−0.1187	−0.2958	−0.1357	−0.3563	0.0317
Avg spread (Mean)	1.0348	0.4604	1.1353	0.2860	0.1331
Std spread (Mean)	0.0000	0.4046	0.1004	0.1066	0.0142
Skew spread (Mean)	0.0251	0.8658	1.6010	0.6978	0.5295
Corr(Density, stability)	−0.4688	−0.4253	−0.3837	−0.7981	0.0275
Corr(Density, avg spread)	0.0296	−0.0003	0.0896	0.7960	0.0229
Autocorr(Density)	0.0034	0.5697	0.2455	0.8174	0.0243
Autocorr(Avg volume)	0.0014	0.3875	0.0760	0.4926	0.0555
Autocorr(Avg spread)	0.9991	0.1624	0.2425	0.9655	0.0031
Objective function value	227.3328	6.5852	4.2407		
Euclidean norm $\|\hat{\boldsymbol{\beta}}_T - \tilde{\boldsymbol{\beta}}_{TS}\|$	6.8563	2.4022	2.0035		
Sup Norm $\|\hat{\boldsymbol{\beta}}_T - \tilde{\boldsymbol{\beta}}_{TS}\|_\infty$	4.4568	1.5217	0.9032		

Notes: The table reports the values of the observed auxiliary statistics $\hat{\boldsymbol{\beta}}_T$ used in the indirect inference estimation along with the HAC robust standard errors, as well as the simulated average of the auxiliary statistics for different model parameterizations: (i) for the estimated parameter vector of the unrestricted model $\hat{\boldsymbol{\theta}}_T$; (ii) for the calibrated vector $\boldsymbol{\theta}^r$ that equals $\hat{\boldsymbol{\theta}}_T$ but sets the effect of monitoring to zero ($\beta_{\phi,1}$=0); and (iii) for the estimated parameter vector of the restricted model without monitoring $\hat{\boldsymbol{\theta}}^r_T$ (with the restriction $\beta_{\phi,1}$=0). The observed statistics are computed on a sample of daily frequency from February 18, 2008, to April 28, 2011, of size $T = 810$. The objective function is a quadratic form with diagonal weight matrix using $S = 24$ simulated network paths, each of length 3000 periods (see Eq. (4.1)). For the different structural parameter vectors, see Table 3. Density is not included in the vector of auxiliary statistics as the density is proportional to average degree.

the effect of expected profitability (expected loan volumes and interest rates) on the search decisions. In this respect, the positive point estimate of 0.85 for λ^y indicates persistent expectations about available bilateral loan volumes. Similarly, the estimated value of 0.93 for λ^B indicates a strong persistence in the expectation of being contacted by a specific borrower. These persistent expectations eventually contribute to the high persistence of bilateral trading relationships. The estimated value for λ^r is considerably lower (0.40), suggesting that new information about bilateral interest rates is more heavily weighted in the expectation formation process, compared to expectations about volumes and contacts which are relatively more persistent. On the other hand, the changes in bank-to-bank credit-risk uncertainty immediately feed into expectations, as the 0.03 estimate for $\lambda^{\tilde{\sigma}}$ indicates. Clearly, the model without monitoring does not include the parameters λ^B and $\lambda^{\tilde{\sigma}}$, which affect the monitoring decisions only through the optimal monitoring policy rule.

Third, the distribution's estimated values of the hyper-parameters of the distribution that characterize banks' individual liquidity shock distributions point toward significant heterogeneity. The estimated log normal distribution implies that there are a few banks with very large liquidity shock variances that are very active market players. Moreover, the notion that some banks structurally provide or demand liquidity is supported by the positive estimate of the mean's variance parameter. Note also the estimated negative correlation parameter, which indicates that banks with a small liquidity shock variance typically have a positive mean.[23] We discuss the role of bank heterogeneity in more detail in Section 5.

In Table 4, we report the coefficients of the linear policy rule for the optimal monitoring levels as implied by the estimated parameters (monitoring is expressed in deviations from steady-state values). It is particularly noteworthy that the optimal monitoring level toward a particular bank depends positively on the expected probability of being approached by this bank to borrow funds during future trading sessions, $\mathbb{E}_t B_{i,j,t+1}$. Indeed, this positive coefficient and the significantly positive effect of search on link formation (endogenous counterparty selection) create the connection between monitoring and search as the source of persistent trading relationships. Moreover, the current state of credit-risk uncertainty positively affects monitoring during the current period. Higher expected future uncertainty, however, reduces these efforts as the

[23] Interestingly, the estimation results of the restricted model without monitoring do not exhibit this negative correlation; instead, there is a larger variance in banks' mean and standard deviation parameters.

expected profitability of interbank lending declines. The positive coefficient on the amount of granted loans shows that banks prefer to monitor those counterparties with whom they expect to trade larger volumes. This finding is intuitive, since the surplus that can be generated by reducing credit-risk uncertainty is larger. Hence, monitoring reacts positively to expectations of increased profits in the future, similar to banks' optimal search decision.

The estimated policy rules for peer monitoring and search imply that shocks to interbank trading profitability lead to an endogenous multiplier effect that works as follows. Suppose there is a positive shock to the bilateral loan (or similarly a positive shock to the link, or a negative shock to the credit-risk uncertainty). In response, banks' expected profitability increases, and banks increase their monitoring and search efforts. As a consequence, more loans are granted and interest rates decrease. These developments feed into banks' expectations about spreads and bilateral link probabilities, which further promotes monitoring and search. As a consequence, the multiplier effect of monitoring and endogenous counterparty selection further drives up the link probability and reduces interest rates. Thus, the initial shock to interbank profitability is reinforced by the interrelationship between control variables, outcomes, and state variables. This basic amplification mechanism is at the core of our model and can explain several features of the observed interbank network that we discuss next.

5. Model analysis

In this section, we use the estimated structural model to study the effects of key frictions on the network structure. Our analysis focuses on assessing the role of private information, gathered through peer monitoring and repeated interactions, in shaping the network of bilateral lending relationships and associated interest rates and volumes. Moreover, we use the model to analyze the effect that changes in the central bank's discount window have on the interbank lending structure.

5.1. Comparison of auxiliary statistics

We first analyze the model's fit, along with the observed and simulated values of the auxiliary statistics under the estimated structural parameter $\hat{\boldsymbol{\theta}}_T$. We benchmark our estimated model against an alternative model parametrization $\boldsymbol{\theta}^r$, where the effects of monitoring on the perception-error variance are restricted to zero ($\beta_{\phi,1} = 0$). By focusing on the monitoring channel. but keeping all other things equal (in particular, the parameters related to banks' liquidity shock distribution and search technology), we evaluate the role of peer monitoring on the network structure and associated bilateral credit conditions from a *ceteris paribus* perspective. Moreover, we compare the fit of the full model to the restricted but re-estimated model without monitoring ($\beta_{\phi,1} = 0$), where all the other parameter values are determined by the data (parameter vector $\hat{\boldsymbol{\theta}}_T^r$).

Table 5 shows how the estimated structural parameter vector $\hat{\boldsymbol{\theta}}_T$ produces an accurate description of the data when compared to the alternative calibrated parameter vector $\boldsymbol{\theta}^r$ without monitoring. First, note the remarkable improvement in model fit compared to the calibrated example. This is brought about by the indirect inference estimation, as judged by (i) the value of the (log) criterion function that is about 54 times smaller for the estimated model, and (ii) the comparison between auxiliary statistics obtained from the observed data, data simulated at the calibrated parameter, and data simulated at the estimated parameters. For instance, the Euclidean norm and the sup norm of the difference between observed and simulated auxiliary statistics are about 3.5 and 5 times larger, respectively, under the calibration without monitoring. Also, when compared with the restricted estimated model without monitoring (parameter vector $\hat{\boldsymbol{\theta}}_T^r$), we find that the overall fit of the estimated model with monitoring provides a better description of the observed data, with the objective function value being only 0.62 as large and the Euclidean and sup norm of the distance between the observed and simulated auxiliary statistics being only 0.83 and 0.59 times as large, respectively.

A closer look at the individual auxiliary statistics confirms the importance of the peer monitoring channel for replicating the network structure and reveals several interesting features of the estimated model.[24] First, it is important to highlight the significant improvement in the fit of the density compared to the calibrated example. In fact, with a density of about 0.02, the estimated model matches the sparsity of the Dutch interbank network very well. Hence, only a few bank pairs trade in the market on a daily basis. Likewise, the proposed structural model provides a very accurate description of the network's high stability, with a value of 0.98. Similarly, with a small value of 0.03, the average clustering coefficient matches the data very well and is a considerable improvement over the calibrated model. Moreover, the estimated model implies that about 6.3% of all links are reciprocal, compared to 8.2% in the observed data.

Second, a comparison of the observed and simulated auxiliary statistics shows that the model well replicates the first three moments of the observed degree distribution.[25] In particular, the estimated model generates a high positive skewness of both the in-degree and out-degree distribution (compare the respective simulated skewness of 2.4 and 2.3 with the observed skewness of 2.8 and 2.4, respectively). Similarly, the standard deviation of both degree distributions are quite accurate, with respective values of 1.7 and 1.7 compared with the observed counterparts of 1.8 and 1.6. Fig. 4 plots the

[24] In the following, we refer to the estimated model as the unrestricted model characterized by $\hat{\boldsymbol{\theta}}_T$ (that is, the estimated model with monitoring).

[25] The density is just a rescaled version of the average degree centrality; we did not include the density in the estimation but show it for convenience in Table 5.

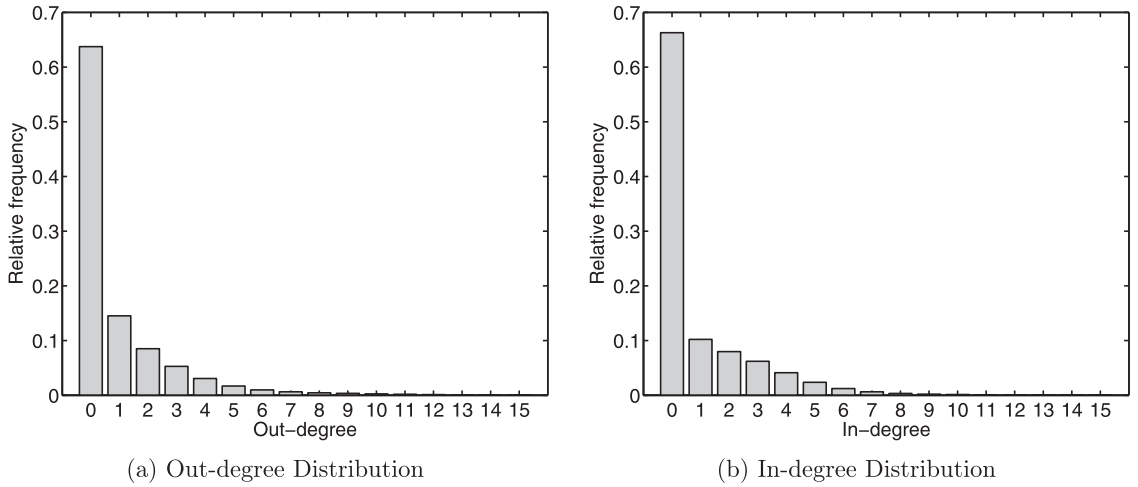

(a) Out-degree Distribution (b) In-degree Distribution

Fig. 4. Degree distribution under the estimated parameter vector $\hat{\boldsymbol{\theta}}_T$. *Notes:* Marginal in- and out-degree distributions computed based on 5000 simulated network paths of size $T = 25$ under the estimated parameter vector $\hat{\boldsymbol{\theta}}_T$. *Source:* Authors' calculations.

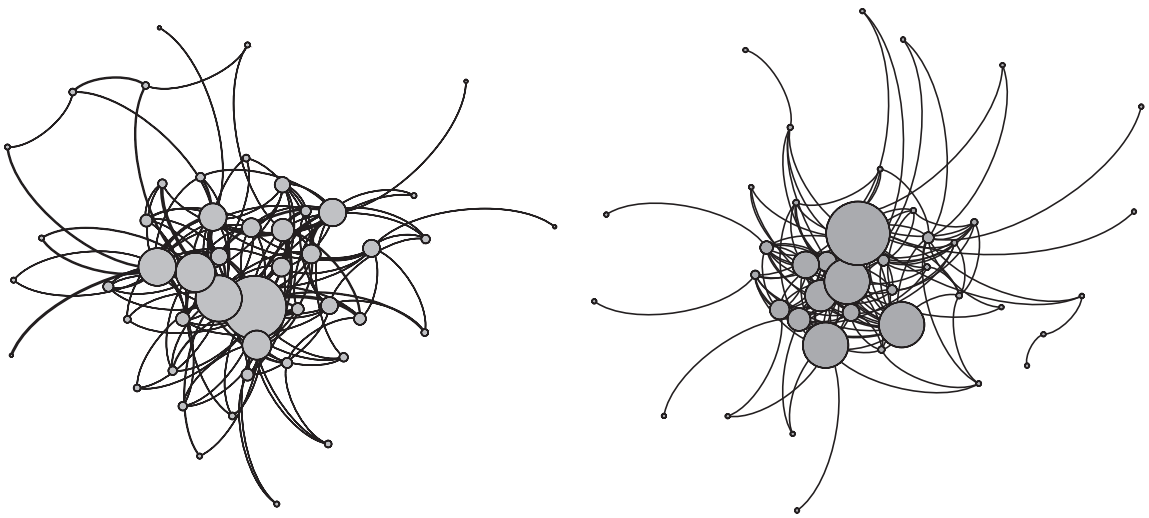

(a) Observed Network **(b) Simulated Network (under $\hat{\boldsymbol{\theta}}_T$)**

Fig. 5. Interbank network market structure for one trading week. *Notes:* Nodes are scaled according to total trading volume. The observed network corresponds to first week in April 2008; simulated network under estimated parameter $\hat{\boldsymbol{\theta}}_T$ is randomly picked realization. Isolated nodes are not shown. *Source:* Authors' calculations.

simulated (marginal) in-degree and out-degree distributions under the estimated model parameters. The figure is the result of a Monte Carlo (MC) analysis based on 5000 different networks, each with $T = 25$. About 65% of all banks have no (zero) trading partners on a daily basis (isolated vertexes); that is, they do not lend or borrow in the market. Moreover, about 60% of active banks have at most two borrowers and two lenders. At the same time, both degree distributions have a very long right tail indicating that there are few banks that borrow and lend from many other banks. Yet it is very rare for banks to have more than 10 counterparties on a daily basis the relative frequency is below 1%.

To illustrate the basic network topology, Fig. 5 depicts the observed interbank network along with a network simulated from the estimated model with monitoring. The figure shows the sparse and concentrated market structure—a few banks at the center of the network trade large volumes on either side of the market (the scale of the nodes relates to lending and borrowing volume). The visualization also highlights the skewed degree distribution of the observed and simulated network that is one key stylized fact of interbank markets. In particular, large banks in the core have multiple counterparties, while small banks typically have few trading partners and are typically connected with banks in the center of the network.

Comparing the estimated auxiliary statistics with those obtained from the calibrated model $\boldsymbol{\theta}^r$ without monitoring shows that monitoring is an important factor in explaining the basic topology of the observed lending network. In contrast to the estimated model with monitoring, the calibrated model fails to specifically match the network's skewed out- and in-degree distributions, with simulated values of 0.45 and 0.33, respectively (note that banks' liquidity shock distributions and all other parameters are held constant). In fact, the estimated model parameterization without monitoring $\hat{\boldsymbol{\theta}}_T^r$ also fails to generate a skewed degree distribution close to the observed one, with out- and in-degree skewness of 1.36 and 1.40, respectively, although all parameters are fully determined by the data. Indeed, as we discuss in detail in the next section, the amplification mechanism of peer monitoring and counterparty selection reinforces the tiered market structure and generates a highly skewed degree distribution.

Third, and key to our analysis, the estimated structural model is able to generate patterns of relationship lending where banks repeatedly interact with each other and trade at lower interest rates. In particular, the positive correlation of 0.60 between past and current bilateral lending activity, that is, the measure of the stability of bilateral lending relationships, matches the observed value of 0.64 very well. Moreover, the model generates a negative correlation of –0.12 between interest rates and past trading (compared with –0.07 for the observed data). As reported in Table 4, monitoring efforts positively depend on the expectation of being approached by a specific borrower. Once a contact between two banks is established, banks positively adjust their expectations and increase monitoring. This greater monitoring effort has a dampening effect on the bilateral interest rate level and thereby makes borrowing more attractive, leading to increased expectations about a contact.

The role of bank-to-bank peer monitoring as the crucial driver behind the observed dynamic structure of the interbank market is also confirmed by comparing the fit of the auxiliary statistics simulated under the calibrated parameter with those of the estimated parameter. Clearly, in the calibrated example where there is no role for monitoring, the stability of bilateral trading relations is low (0.23), and past trading has no effect on current prices, as the effect of trading activity in reducing uncertainty ($\beta_{\phi,2}$) is small and insignificant. In contrast, the estimated model without monitoring generates some relationship lending (–0.16), as the estimated value of $\beta_{\phi,2}$ is larger than in the calibration without monitoring. However, in the calibrated model, the simulated values for the stability of bilateral trading relationships are smaller (0.43), compared with the observed and simulated values of the full model (0.64 and 0.60, respectively), highlighting the importance of the monitoring channel for the persistence of bilateral trading relationships in the market.

Moreover, our estimated model with monitoring—similarly to the estimation results for the restricted model—replicates rather well the mean and skewness of the distribution of (log) volumes of granted loans. Also, the standard deviation points toward heterogeneity in bilateral loan amounts, although the simulated value is not as large as the observed value. The distribution of the potential bilateral volumes depends on the bank-specific liquidity shocks in Eq. (5). However, the decision to lend is endogenous, and hence the distribution of granted loans also depends on other model parameters. Note also that the estimated model does a worse job in explaining the observed average interest rate level, while it nicely captures the cross-sectional standard deviation of spreads that in our model is related to heterogeneous counterparty risk perceptions. Further, the skewness of the cross-sectional interest rate distribution has the correct sign but is twice as large as the observed value.[26]

Finally, we find that our estimated model is able to generate some autocorrelation in the density (0.25) and the average interest rate of granted loans (0.24), in contrast to the average volume of granted loans. Clearly, the estimated values are not as high as the observed values (0.81 and 0.97, respectively). However, there are no common factors in the model, and all shocks are *iid*. The only persistent processes are at the bank-to-bank level: credit-risk uncertainty and the bank-to-bank-specific expectations. Hence, the generated autocorrelation in these aggregate figures results from the same banks trading with each other in subsequent periods. Similarly, the model also generates a negative correlation between the density and the stability, and a positive correlation between density and average spreads. Thus, when there are fewer loans granted, the average interest-rate spread of these loans decreases. In our model, this happens because when counterparty-risk uncertainty is high, only bank pairs with low uncertainty (and hence low spreads) continue to trade.

5.2. Bank heterogeneity and lending relationships

In our model, heterogeneous liquidity shock distributions are the only source of bank heterogeneity. Yet these shocks are important in determining the exogenous volumes of granted loans. As banks' monitoring and search efforts depend on expected loan volumes, the heterogeneous liquidity shock distributions determine the distribution of the multiplier effects from monitoring that are crucial in matching the basic network structure of the interbank market, such as the high skewness of the degree distribution as described in the previous subsection. In our model, the distribution of liquidity shocks in the banking system is characterized by the probabilistic structure described in Section 3.

Fig. 6 plots the joint distribution of the bank-specific mean μ_{ζ^i} and the standard deviation σ_{ζ^i} of the liquidity shocks, as implied by the estimated structural parameters $\hat{\mu}_\mu = 0$, $\hat{\sigma}_\mu = 1.99$, $\hat{\mu}_\sigma = 1.94$, $\hat{\sigma}_\sigma = 1.98$, and $\hat{\rho}_\zeta = -0.78$. First, most probability mass is located around $\mu_{\zeta^i} = 10$ and at small values of σ_{ζ^i}. Hence, the median bank has small liquidity shocks

[26] Recall that the model abstracts from any bank heterogeneity beyond differences in liquidity shocks; in particular, differences in balance sheet strength or heterogeneous outside options. Moreover, in the current model there is no room for excess liquidity that might affect the level of interest rates.

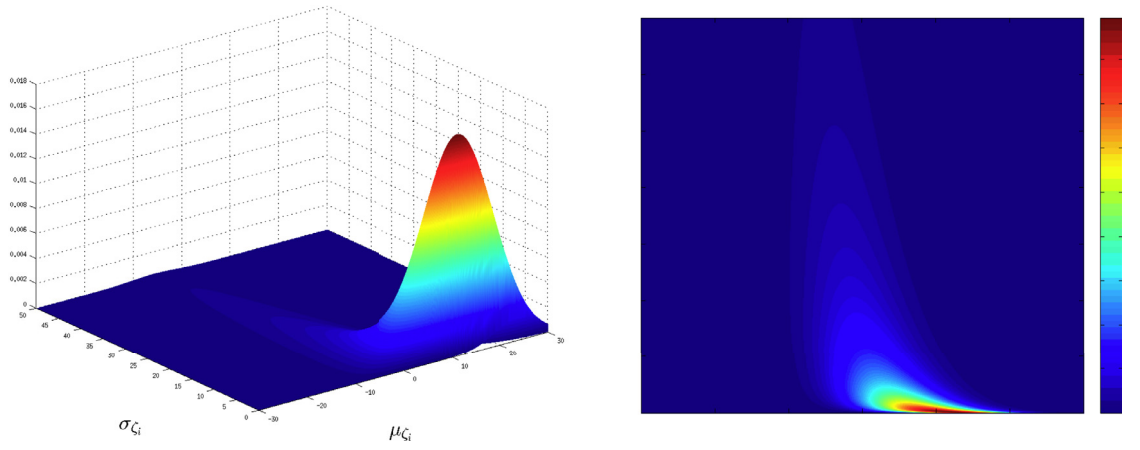

(a) Density (b) Contour Plot

Fig. 6. Liquidity shock distribution under estimated model parameter. *Notes:* Joint distribution of mean (μ_{ζ^i}) and standard deviation (σ_{ζ^i}) of banks' liquidity shock distributions and contour plots as implied by the estimated model parameters. *Source:* Authors' calculations.

that on average are positive but close to zero. Second, the distribution of $\mu_{\zeta i}$ is more dispersed for low values of $\sigma_{\zeta i}$. Thus, for banks with a small variance parameter of the liquidity shock distribution (small banks), there is higher heterogeneity with respect to their mean parameter $\mu_{\zeta i}$. Third, the contour plot reveals that the distribution has a a parabolic form. In particular, small banks with very small-scale liquidity shocks typically tend to have a liquidity surplus, while banks with very large-scale shocks typically have a negative mean, indicating a liquidity deficit. This relationship is driven by the correlation parameter ρ_ζ that we estimate to be -0.78. Finally, the long tail in the dimension of σ_{ζ^i} shows that just a few banks have very large liquidity shock variances.

The estimated bank heterogeneity has important consequences for pairwise credit availability and conditions, as well as for search and monitoring expenses. In Fig. 7, we show the interbank activity during one five-day business week for 50 randomly drawn liquidity shock parameters (associated with 50 banks). Each bank is indicated by a black dot, and its position in the $\mu_\zeta - \sigma_\zeta$ plane is given by the values of the bank-specific mean and standard deviation parameters $(\mu_{\zeta i}, \sigma_{\zeta i})$. The figure reveals that small banks (small liquidity-shock variance) typically provide liquidity to the interbank market, particularly to big banks (those that on average have a positive demand for liquidity) or small banks with complementary liquidity shocks.[27] Market intermediation emerges as big banks (money-center banks) simultaneously act as lenders and borrowers. For small banks, it is most efficient to trade with big banks that have large liquidity shocks than with banks with small liquidity shocks. Moreover, big banks form a tightly interconnected core where each member of the core has reciprocal lending relationships (solid blue lines) with other core banks (see the core-periphery analyses by Craig and von Peter, 2014; in 't Veld and van Lelyveld, 2014). Clearly, on average big banks trade larger loan volumes than small banks as a result of their larger-scale liquidity shocks.

We next present more rigorous Monte Carlo (MC) evidence to analyze the role of bank heterogeneity as the fundamental source of persistent trading opportunities. For this purpose, we simulate 5000 network paths and for each draw sort the lender banks in increasing order according to their variance parameter $\sigma_{\zeta i}$ and sort the borrower banks according to their mean parameter μ_{ζ^i} in increasing order. Hence, we compute the order statistics of both parameters. We then simulate for each draw 25 periods and compute the mean link probability, mean volume, and spreads of granted loans as well as the mean search and monitoring efforts between the lender's order statistics and the borrower's order statistics of all possible bank pairs.

Fig. 8 shows the results of the MC analysis. Panel (a) depicts the mean granted-loan volumes for different bank pairs. In particular, we see that banks with a structural liquidity deficit (on the left of the horizontal axis) are borrowing larger amounts than banks with a structural liquidity surplus (on the right of the horizontal axis). Both types of banks borrow larger volumes from big banks with a large variance parameter (on the top of the vertical axis). Due to the negative correlation parameter ρ_ζ, banks with a low-order statistic $\mu_{\zeta(i)}$ are typically big banks, and thus borrowing volumes with other big banks (with large $\sigma_{\zeta(i)}$) are high. Similarly, the mean traded-volumes are low for banks with a structural liquidity surplus and lender banks with a small-scale variance parameter – see the blue region in Panel (a).

As exogenously determined by the distribution of liquidity shocks, the distribution of loan volumes affects the monitoring decisions that eventually affect the prices at which bank pairs trade liquidity (see Panels (c) and (e)). Those bank

[27] This result is in line with similar empirical findings by Furfine (1999) and Bräuning and Fecht (2017), among others, that small banks are net lenders in the interbank market.

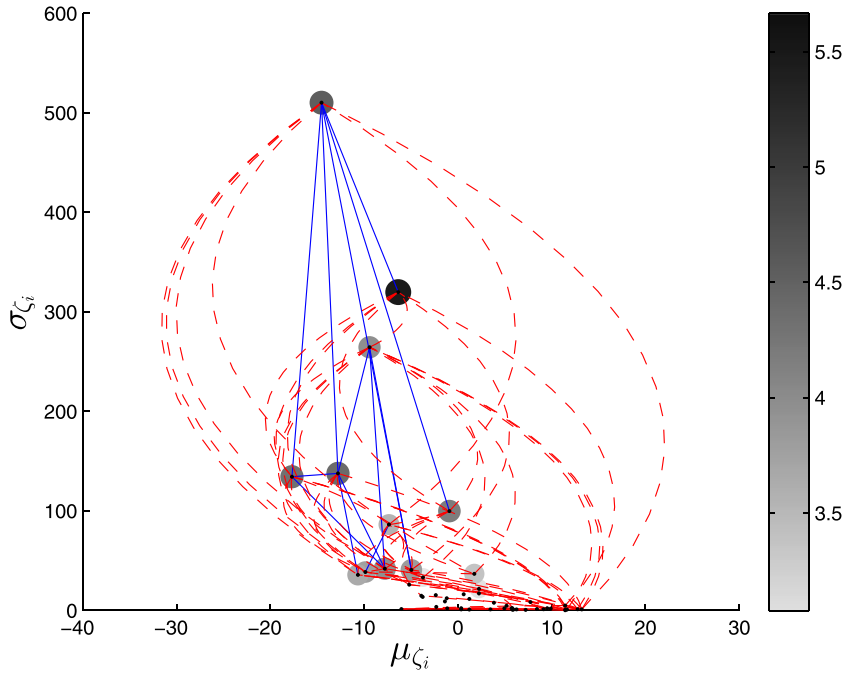

Fig. 7. Simulated interbank activity for one trading week. (For interpretation of the references to color in this figure legend, the reader is referred to the web version of this article.) *Notes:* A bank's position in the $\mu_\zeta - \sigma_\zeta$ plane is given by the mean and standard deviation parameters $(\mu_{\zeta^i}, \sigma_{\zeta^i})$. Node shading relates to average log loan volume per bank (right scale). For each node, incoming links are shown as dashed red lines coming from the right; outgoing links leave nodes from the left (counterclockwise). Solid blue lines represent reciprocal links. *Source:* Authors' calculations.

pairs that can exchange large loan amounts (either because they have a large liquidity shock variance or because on average they have complementary shocks) engage in more monitoring activity and trade at lower spreads (see the parabolic-shaped contour plots). Again, we see that the very large banks engage in high monitoring efforts and trade with each other at very low interest rates (up to 40 basis points lower than high-spread pairs). Hence, these core banks are not only highly interconnected, but the credit-risk uncertainty among these banks is very low (Panel (f)). Due to the interrelationship between monitoring and search, low-interest regions in the figures correspond to bank pairs where search levels are high, leading to high probabilities of successful linkages (see Panel (b)). Moreover, borrowers with a structural liquidity deficit obtain larger loan volumes at lower prices when borrowing from large banks compared with small banks. This discrepancy further highlights the role that intermediation plays in the estimated model. Intermediaries have less credit-risk uncertainty about their borrowers due to higher monitoring intensities, and in turn borrowers have lower credit-risk uncertainty about intermediary banks because lenders direct monitoring efforts toward those borrower banks. Hence, this behavior gives rise to the network's tiered structure, which results from differences in liquidity shocks, reinforced by the presence of credit-risk uncertainty and peer monitoring, leading to different interest rates.[28]

5.3. Dynamic responses to credit risk uncertainty shocks

In this section, we analyze how the dynamics of the estimated network model are affected by shocks to the perception-error variance. To account for the uncertainty about the precise latent liquidity shock distributions, we perform a simulation study by first drawing the properties of each bank (as described by the parameters μ_{ζ^i} and σ_{ζ^i}) and then calculating a set of key network statistics for 25 time periods. This procedure is then repeated in a Monte Carlo setting with 5000 replications. In all the simulated structures, we impose a large positive shock to the perception-error variance in period $t = 4$ (thus affecting the perception-error variance in $t = 5$) to investigate how our key network statistics react to increases in credit-risk uncertainty.

The solid lines in Fig. 9 depict the mean responses across all network structures to an extreme 10 standard deviation shock in credit-risk uncertainty; that is, we impose $u_{i,j,4} = 10\ \forall i, j$. In this figure, the interquartile range (dotted lines) essentially reflects the uncertainty about the exact network structure as described by the unobserved liquidity shock distributions. For instance, the interquartile range of the mean network density is between 0.014 and 0.023, and the mean is about

[28] Fecht et al. (2011) document that the price that banks pay for liquidity depends on the distribution of liquidity across banks.

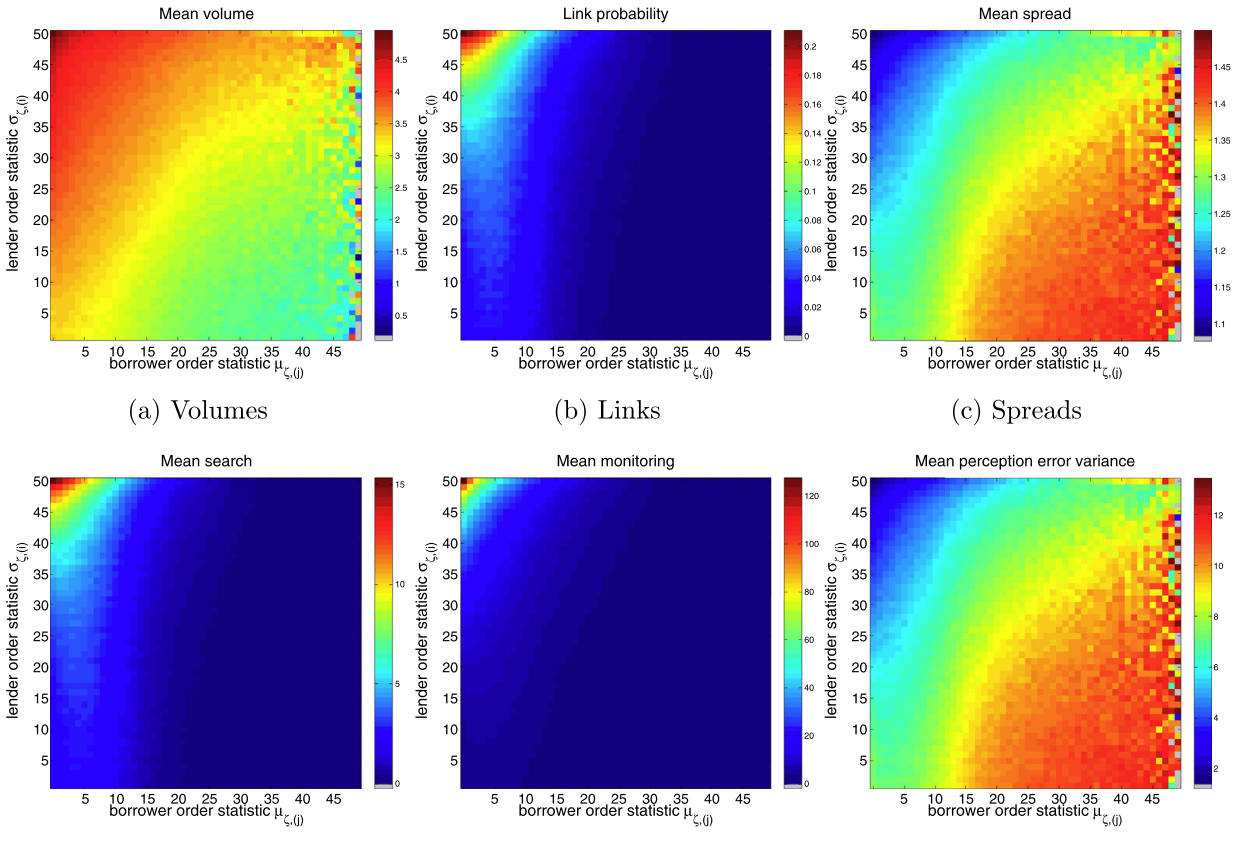

Fig. 8. Bank heterogeneity and trading relationships. (For interpretation of the references to color in this figure, the reader is referred to the web version of this article.) *Notes:* The order statistics for the lender variance parameters $\sigma_{\zeta^{(i)}}$ are depicted on the vertical axis, while the order statistics for the borrower mean parameters $\mu_{\zeta^{(i)}}$ are depicted on the horizontal axis, that is, lender banks are ordered by variance parameter σ_{ζ^i} such that $\sigma_{\zeta^{50}} > \sigma_{\zeta^{49}} > \cdots > \sigma_{\zeta^1}$, and borrower banks are ordered by mean parameter such that $\mu_{\zeta^{50}} > \mu_{\zeta^{49}} > \cdots > \mu_{\zeta^1}$. The results are based on 10,000 MC repetitions, each of length $T = 100$. *Source:* Authors' calculations.

0.019, depending on the precise network structure.[29] In the top panel, we show that at the time of the shock to the credit-risk uncertainty, the network density drops by more than 75%. Both the density and total volume remain at low levels, and 20 trading days after the shock they still remain at only 50% of their pre-crisis values. Moreover, the log of total transaction volume plummets by more than 50% as a result of reduced trading activity. At the same time, we observe an increase in the average (log) volume of granted loans compared with pre-shock loan levels and an increase in the network stability one period after the shock. Similarly, both in-degree and out-degree distributions become more positively skewed, and there is over a two-fold increase in reciprocity.[30] Hence, the network shrinks and trading becomes more concentrated among the highly interconnected core banks.

These changes are driven by the fact that in the aftermath of the shock, some bank pairs that had been actively trading cease this activity amid deteriorating risk assessments of borrowers. As the implied interest rate spreads explode, lending in the interbank market becomes unattractive for some pairs compared with the outside option. These loans are substituted by increased recourse to the central bank's standing facilities (not shown), which moves inversely to the density and total transaction volume in the interbank market. In fact, the increased average loan volume shows that for $t = 5$, a large fraction of trading bank pairs exchange larger volumes (due to their size and/or complementarity of liquidity shocks). As discussed in the previous section, these are bank pairs where monitoring is particularly profitable and bank-to-bank uncertainty is low, rendering interbank lending more attractive than the outside option, even after the shock. Yet, those trades that do occur also are associated with increased spreads due to higher uncertainty; the average spread of granted volumes increases by about 6 basis points right after the shock. Thus, the compositional effects do not immediately outweigh the uncertainty-

[29] For any fixed structure of liquidity shocks, the interquartile range is much tighter around the mean response.

[30] The lower bound remains at zero because for some network structures interbank lending breaks down completely, leading to zero reciprocity.

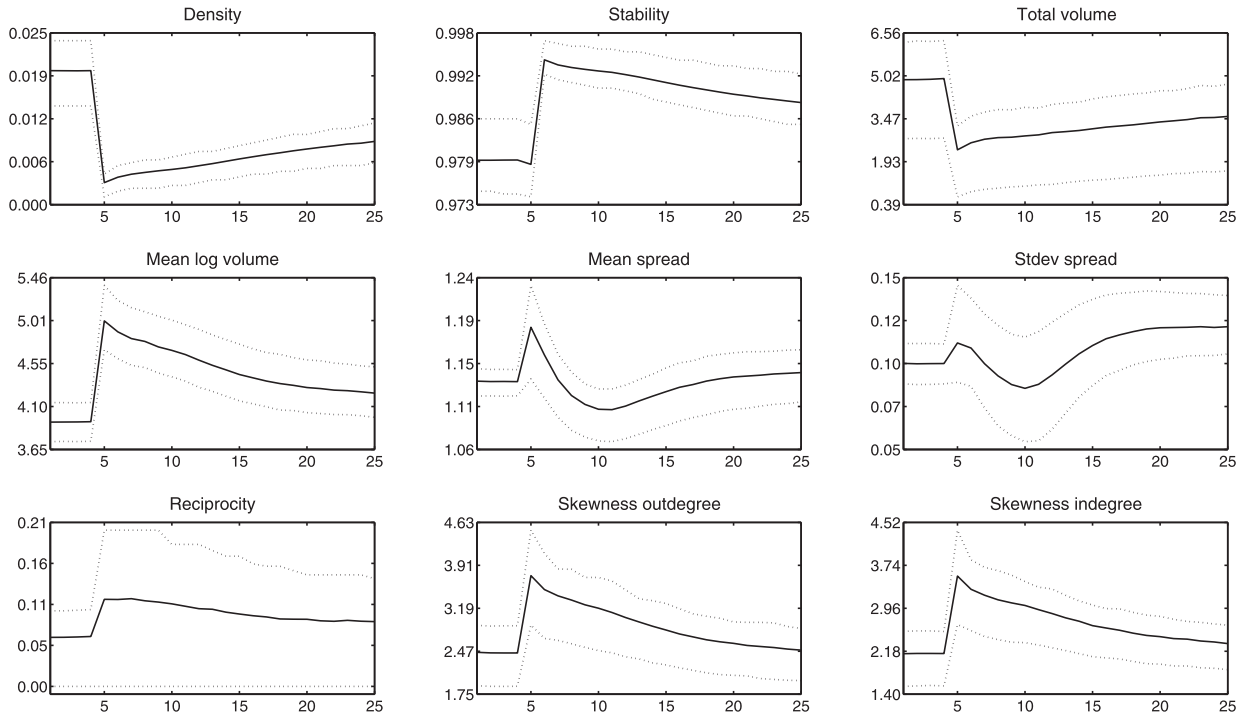

Fig. 9. Impulse responses to a shock in credit-risk uncertainty. *Notes:* Simulated impulse responses to a common 10 standard deviations shock in credit-risk uncertainty in period four. Results are based on 5000 MC repetitions. The solid line is the mean impulse response, and the dotted lines refer to the interquartile range across all network structures. Total volume is in billions, and mean volume is the mean log volume (in millions) of granted loans. *Source:* Authors' calculations.

induced increases in interest rates. However, about two periods after the shock, the average spread of the interbank trades that do occur return to the initial pre-shock levels, and a further decrease can be observed until about period 10 when the average rate of traded loans is below the pre-shock level. A similar pattern can be observed for the cross-sectional standard deviation of interest rates. While it falls to 0.11 as the shock hits, it decreases to about 0.09 in period 10 when the mean spreads are lowest, and then for an extended period of time rises to a value higher than pre-shock levels.

Fig. 10 depicts how the impulse responses for the banks' expectations and control variables act as crucial drivers for the changes in the observable network statistics. Again, the solid line refers to the mean and the dotted lines refer to the interquartile ranges that represent the uncertainty about the latent network structure. The top left panel shows how the mean credit-risk uncertainty induced by the shock peaks in period five. Clearly, the increase in the mean credit-risk uncertainty translates into an increase in the mean expectations about future credit-risk uncertainty that displays similar behavior, although at lower values. As a consequence of the higher expected uncertainty after the shock (that directly translates into higher bilateral equilibrium rates), the expected profitability of interbank borrowing decreases as the spread that can be earned in the interbank market compared to discount window borrowing declines. This lower degree of profitability leads borrower banks to invest less in counterparty search, further bringing down trading in the interbank market. The impaired funding conditions due to higher credit-risk uncertainty only feed gradually into borrowers' expectations about interbank profitability, as borrowing banks only update their expectations once they are in contact with a lender. Therefore, the mean search effort by borrowers gradually declines until it reaches a minimum in period 10. Moreover, this reduced search effort is reflected in lenders' expectations about future contacting probabilities, which gradually decline from period 5 onward until the end of the plotted sample (although the decrease in the mean expectation is arguably small).

Moreover, as a response to the increased perception-error variance, banks adjust their monitoring expenditures from about 4500 euros on average (per bank-pair) downward to 2000 euros. This decrease, which contributes to the prolonged period of interbank trading inactivity that prevents a fast market recovery, is driven by several channels. First, from the estimated linear policy rules, we find that banks increase monitoring as a response to higher credit-risk uncertainty. However, at the same time, they decrease peer monitoring to adjust to future expected uncertainty. Because the estimated exponentially weighted moving average (EMWA) parameter is low, these expectations closely follow the actual credit-risk uncertainty that has quite persistent dynamics. In sum, the negative effect of future uncertainty dominates such that the overall mean effect of this large 10 standard deviation shock is negative. Second, due to lower search efforts, the gradual decrease in the probability of expected future contact further dampens banks' monitoring expenditures and prevents the interbank market from making a faster recovery.

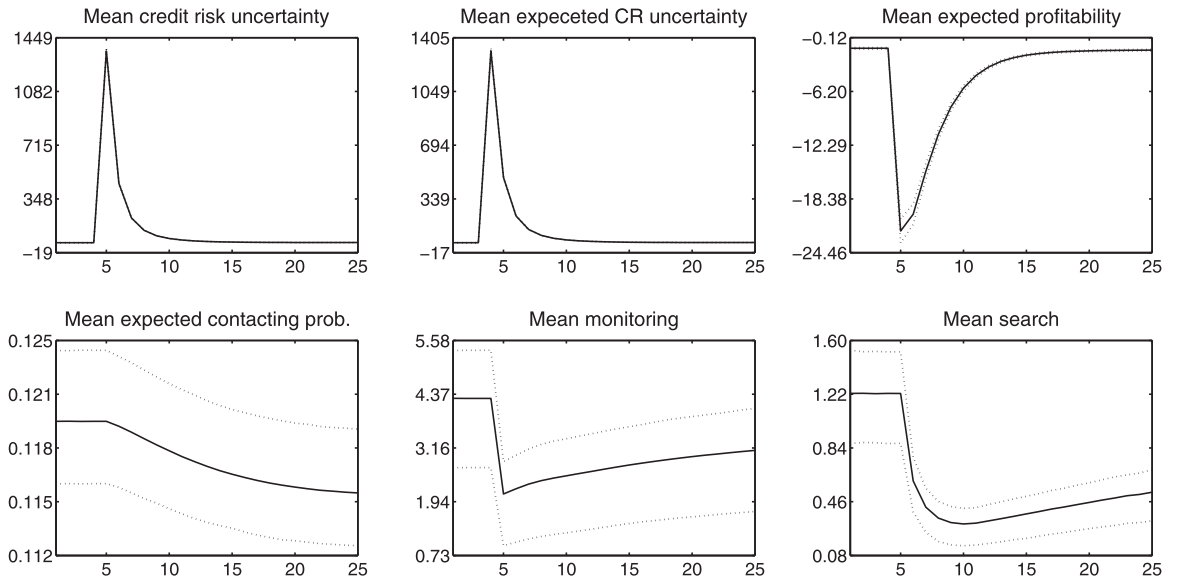

Fig. 10. Impulse responses to a shock in credit-risk uncertainty. *Notes:* Simulated impulse responses to a common 10 standard deviation shock in credit-risk uncertainty in $t = 4$. Results are based on 5000 MC repetitions. The solid line is the mean impulse response, and the dotted lines refer to the interquartile range across all network structures. Expectations are in deviations from steady-state values. Monitoring and search expenditures are in thousands of euros. *Source:* Authors' calculations.

5.4. Monetary policy analysis: the interest rate corridor

A key parameter of the model is the central bank's interest rate corridor, as it determines the price of the outside options to interbank lending. We next analyze how changes in the corridor's width affect the interbank lending network and associated credit conditions.

Fig. 11 shows how changes in the width of the corridor produce significant changes in the structure of the interbank lending network that are driven by changes in banks' monitoring and search efforts. Again, the uncertainty captured by the interquartile range largely captures the uncertainty about the precise latent distribution of liquidity shocks in the banking system. The most striking feature in Fig. 11 is that an increase of roughly 100% in the width of the central bank's interest rate corridor (from 1 to 2 percentage points) produces over a three-fold increase in the mean network density (the average number of daily trades), going from a roughly 1% density to one that is over 3%. Furthermore, at a corridor width of 2 percentage points, the lower bound of the interquartile range across all network structures is larger than the upper bound on the interquartile range across network structures at a corridor width of 1 percentage point. This analysis shows that these effects on credit conditions are highly significant and that the interest rate corridor width plays an important role in the intensity of interbank activity.

Fig. 11 illustrates a second important feature of the model—due to its nonlinear nature, the multiplier's value is not constant over the range of corridor widths. In particular, Fig. 11 shows that the multiplier's value decreases with the corridor width. Indeed, a 10 basis point increase of the bound has a much larger relative effect on the network density for lower corridor widths compared to larger ones. For instance, increasing the bound from 1.0 to 1.25 percentage points leads to a relative increase of about 45% in density, while an increase from 1.75 to 2.0 percentage points leads to a relative increase in density of about 28%. The presence of this multiplier, as well as its nonlinearity, are both explained by the role that monitoring and search efforts play in the interbank market. Similar to the Keynesian spending multiplier, the effects of a change in the width of the interest rate bounds can also be decomposed into *(i)* an immediate short-run effect, and *(ii)* a long-run effect that results from feedback loops between the effect of monitoring and search on loan outcomes, and expectations about credit conditions.

Consider a decrease in the width of the interest rate corridor. In response to this shock, the interbank market immediately shrinks, as a fraction of potential loans are no longer profitable given the tighter new bounds. The immediate mechanical effect is that part of the interbank market switches to lending and borrowing from the central bank, which now plays a more important role in credit markets. This immediate short-run effect, however, only constitutes a fraction of the total long-run multiplier effect. Indeed, given that the possibilities of interbank trading are now smaller, expected future profits are reduced, and the incentive to search for and monitor partners is diminished. This reduction in search and monitoring (depicted in Fig. 11) will further reduce the mean density and mean traded-volumes in the interbank market. In turn, these reductions force banks to revise downward the expected profitability of monitoring and search efforts, further lowering these mean variables. This spiraling negative effect that defines the multiplier eventually will bring the market to a new operating

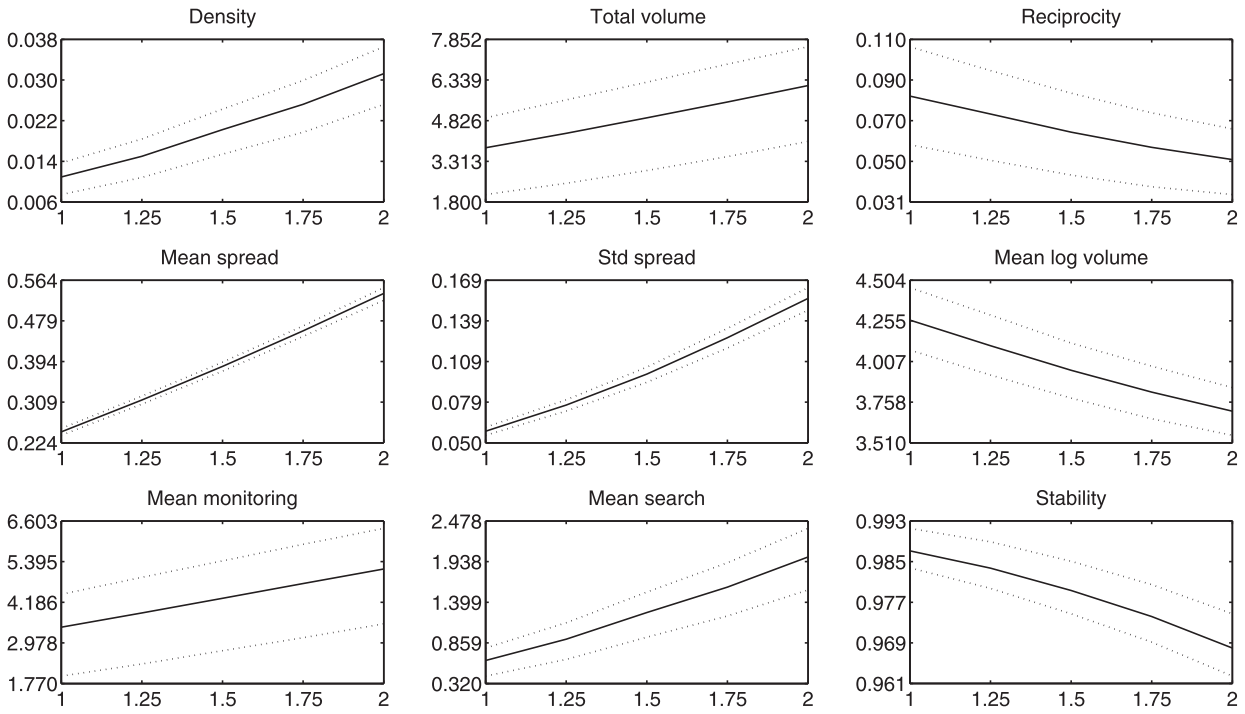

Fig. 11. Changes in the central bank's interest rate corridor width. *Notes:* Simulated mean and interquartile range of key network statistics and mean monitoring and mean search per bank over alternative interest corridor width. Total volume is in billion euros. The Monte Carlo results are based on 5000 networks each with $T = 25$. *Source:* Authors' calculations.

level that may be orders of magnitude lower than the observed values prior to the imposition of the tighter interest rate bounds.

Similarly, an increase in the size of the interest rate corridor leads to wider participation in the interbank market, again fostered by banks' increased levels of monitoring. Moreover, from Fig. 11 we find that with a wider interest rate corridor, both the mean spread of granted loans (relative to the center of the corridor) as well as the cross-sectional standard deviation increase, while the average (log) volume traded decreases. The changes in these market outcomes are driven by bank pairs that did not trade under the narrower interest rate corridor but instead preferred to deposit funds at the central bank. Although interest rates remain high after the corridor is widened, trading becomes profitable for those bank pairs, driving up the average rate and the standard deviation of granted loans. Similarly, the trading network's reciprocity and stability decrease because with a wider corridor, trading becomes more attractive for those smaller banks that only occasionally seek to access the interbank market.

Hence, if the central bank wishes to get tighter control over the traded interbank rates by narrowing the interest rate corridor, it has to expect further adverse effects on interbank lending activity triggered by a reduction of counterparty search and monitoring. On the other hand, if the central bank wants to foster an active decentralized interbank lending market as a means to explore the benefits obtainable from peer monitoring, it is essential to consider policies that increase the rate differential between the interbank market and the standing facilities for depositing and lending funds. Only then is the interbank market profitable enough to encourage intense peer monitoring and search among banks. Regardless of whether the central bank wants to encourage or discourage using the interbank market, the multiplier effect should be taken into account when considering policy changes.

6. Conclusion

In this paper, we propose and develop a structural micro-founded network model for the unsecured OTC interbank market where banks can lend and borrow funds to smooth liquidity shocks or resort to using the central bank's standing facilities. Banks choose which counterparties to approach for bilateral Nash bargaining about interest rates and set their monitoring efforts to mitigate asymmetric information problems about counterparty risk. We estimate the structural model's parameters using a novel indirect inference estimator based on network statistics for the Dutch unsecured overnight interbank lending market running from mid-February 2008 through April 2011.

Our model-based analysis shows that the prevailing bank-to-bank uncertainty and peer monitoring levels interact with counterparty search to generate an amplification mechanism that can replicate the key characteristics of interbank markets.

First, banks form long-term lending relationships that are associated with improved credit conditions. Second, the lending network exhibits a sparse core-periphery structure. Moreover, our dynamic analysis shows that shocks to credit-risk uncertainty can diminish lending activity for extended periods of time.

Based on our estimation results, we discuss the implications for monetary policy. In particular, we show that in order to foster trading activity in unsecured interbank markets and exploit the benefits from peer monitoring, an effective policy measure is to widen the bounds of the interest rate corridor. The full effects of a wider corridor are due to both a direct effect and a nonlinear indirect multiplier effect triggered by increased monitoring and search activity among banks.

In addition to the presented robustness of our results to several forms of model misspecification, we believe in future analysis it would be important to incorporate other features in the model and see if and how our presented results change. For example, the model presented in this paper abstracts from correlated liquidity shocks or changes in the operational framework of monetary policy throughout the sample period (e.g., allotment policy). Similarly, considering endogenous pair-specific bargaining power seems like a relevant extension that could potentially affect our estimation results. Including these more realistic features in the model as well as running additional robustness checks is beyond the scope of this paper, but it would be insightful to further evaluate the impact of monitoring and search in interbank networks and derive policy implications.

Acknowledgments

We thank Henrique Basso, Darrell Duffie, Lucy Gornicka, Siem Jan Koopman, Marco van der Leij, Andre Lucas, Patrick McGuire, Albert Menkveld, Joe Peek, Gabriel Perez Quiros, Gerhard Rünstler and Hyun Song Shin for comments. Participants at seminars at De Nederlandsche Bank, Deutsche Bundesbank, the Bank of England, the Bank for International Settlements, the Duisenberg School of Finance, the ECB Money Market Workshop, the Cambridge Workshop on Financial Risk and Network Theory, the 7th Annual SoFiE Conference, the 1st Annual IAAE Conference, the Banque de France – SoFiE Conference on Systemic Risk and Financial Regulation, the GENED Workshop on Networks in Macroeconomics and Finance, the Atlanta Fed Liquidity Conference, and the 2016 ASSA/IBEFA meetings also provided useful feedback. We thank Elizabeth Murry for providing language and grammar suggestions and comments. Blasques and Bräuning gratefully acknowledge financial support from the Netherlands Organisation for Scientific Research (NWO) and the SWIFT institute. The opinions expressed in this paper do not necessarily reflect those of the Federal Reserve Bank of Boston, the Federal Reserve System, De Nederlandsche Bank, or the Eurosystem.

Appendix A. Model solution

The variable $l_{i,j,t} = B_{i,j,t} \cdot \mathbb{I}(r_{i,j,t} \leq r) \cdot \mathbb{I}(y_{i,j,t} > 0)$ introduces a discontinuity that prevents us from obtaining analytic optimality conditions of the original optimization problem stated in Eq. (7). Although numerical solutions are theoretically possible, these would make simulation and estimation prohibitively time-consuming given the high dimensional problem.

We therefore consider an approximate smooth problem where we replace the original problem's step functions ($\mathbb{I}(r_{i,j,t} \leq r)$) by a continuously differentiable logistic function $I(r_{i,j,t}) = \frac{1}{1+\exp(-\beta_I(r-r_{i,j,t}))} =: I_{i,j,t}$. Note that for a growing scale parameter, the logistic transformation approximates the step function arbitrarily well. Without changing the notation, we redefine $l_{i,j,t} = B_{i,j,t} I_{i,j,t}$, where we dropped the factor $\mathbb{I}(y_{i,j,t} > 0)$ without changing the optimization problem, as by the construction of $y_{i,j,t}$, funds are exchanged only if i has a surplus and j a deficit.

We can solve this approximate optimization problem using the well-understood calculus of variations, the most widely applied method to solve constrained dynamic stochastic optimization problems in structural economics (see, for example, DeJong and Dave, 2006; Judd, 1998). Substituting out all definitions in the objective function, except for the law of motion for $\tilde{\sigma}^2_{i,j,t}$, we can write the Lagrange function of the optimization problem with multiplier $\mu_{i,j,t}$ given by

$$\mathcal{L} = \mathbb{E}_t \sum_{s=t}^{\infty} \left(\frac{1}{1+r^d}\right)^{s-t} \sum_{j=1}^{N} \pi_{i,j,t}(m_{i,j,t}, s_{j,i,t}, \tilde{\sigma}^2_{i,j,t}) + \mu_{i,j,t}(\xi(m_{i,j,t}, \tilde{\sigma}^2_{i,j,t}) - \tilde{\sigma}^2_{i,j,t+1}),$$

where we make explicit the arguments that can be influenced by bank i's decision. The Euler equations that establish the first-order-conditions to the infinite-horizon nonlinear dynamic stochastic optimization problem can then be obtained by optimizing the Lagrange function with respect to the control variables and the dynamic constraints (see, for example, Heer and Maußner, 2005).

Under usual regularity conditions, the integration and differentiation steps can be interchanged, and we obtain

$$\frac{\partial \mathcal{L}}{\partial m_{i,j,t}} = 0 \;\Leftrightarrow\; \mathbb{E}_t\left[\frac{\partial \pi_{i,j,t}}{\partial m_{i,j,t}} + \mu_{i,j,t}\frac{\partial \xi_{i,j,t}}{\partial m_{i,j,t}}\right] = 0$$

$$\frac{\partial \mathcal{L}}{\partial \tilde{\sigma}^2_{i,j,t+1}} = 0 \;\Leftrightarrow\; \mathbb{E}_t\left[-\mu_{i,j,t} + \frac{1}{1+r^d}\left(\frac{\partial \pi_{i,j,t+1}}{\partial \tilde{\sigma}^2_{i,j,t+1}} + \mu_{i,j,t+1}\frac{\partial \xi_{i,j,t+1}}{\partial \tilde{\sigma}^2_{i,j,t+1}}\right)\right] = 0$$

$$\frac{\partial \mathcal{L}}{\partial s_{i,j,t}} = 0 \;\Leftrightarrow\; \mathbb{E}_t\left[\frac{\partial \pi_{i,j,t}}{\partial s_{i,j,t}}\right] = 0$$

$$\frac{\partial \mathcal{L}}{\partial \mu_{i,j,t}} = 0 \;\Leftrightarrow\; \mathbb{E}_t\left[\tilde{\sigma}^2_{i,j,t+1} - \xi\left(\phi_{i,j,t}, \tilde{\sigma}^2_{i,j,t}\right)\right] = 0,$$

for all counterparties $j \neq i$ and all t. Substituting out the Lagrange multipliers and taking fixed values at time t out of the expectation gives the Euler equation for the optimal monitoring path that equates marginal cost and discounted expected future marginal benefits of monitoring,

$$\frac{1}{1+r^d}\frac{\partial \xi_{i,j,t}}{\partial m_{i,j,t}}\mathbb{E}_t\left(\frac{\frac{\partial \xi_{i,j,t+1}}{\partial \tilde{\sigma}^2_{i,j,t+1}}}{\frac{\partial \xi_{i,j,t+1}}{\partial m_{i,j,t+1}}} + \frac{\partial \pi_{i,j,t+1}}{\partial \tilde{\sigma}^2_{i,j,t+1}}\right) = 1. \tag{13}$$

Unlike monitoring expenditures, search becomes effective in the same period it is exerted and does not directly alter future matching probabilities via a dynamic constraint. Thus, the first-order condition for the optimal search path is given by

$$\frac{\partial}{\partial s_{i,j,t}}\mathbb{E}_t\left[(r - r_{j,i,t})y_{j,i,t}l_{j,i,t}\right] = 1, \tag{14}$$

leading to the usual condition that the expected marginal benefit equals the marginal cost in each period without any discounting. Since the first-order conditions hold for all $j \neq i$ and the marginal cost of monitoring and search is the same across all j, the conditions also imply that (discounted) expected marginal profits of monitoring and search must be the same across different banks j.

The transversality condition for the dynamic problem is obtained as the limit to the endpoint condition from the corresponding finite horizon problem and requires that

$$\lim_{T\to\infty}\mathbb{E}_t\left[\left(\frac{1}{1+r^d}\right)^{T-2}\frac{\partial \pi_{i,j,T-1}}{\partial m_{i,j,T-1}} - \left(\frac{1}{1+r^d}\right)^{T-1}\frac{\partial \pi_{i,j,T}}{\partial \tilde{\sigma}^2_{i,j,T}}\frac{\partial \xi_{i,j,T-1}}{\partial m_{i,j,T-1}}\right] = 0.$$

Thus, in the limit the expected marginal cost of investing in monitoring must be equal to the expected marginal return.

Eqs. (13) and (14) constitute the first-order conditions to banks' approximate optimization problem. From the first-order condition for the optimal search expenditure in Eq. (14) we get

$$\begin{aligned}
&\frac{\partial}{\partial s_{i,j,t}}\mathbb{E}_t\left[(r - r_{j,i,t})y_{j,i,t}l_{j,i,t}\right] = 1 \\
\Leftrightarrow\; &\frac{\partial}{\partial s_{i,j,t}}\mathbb{E}_t\left[(r - r_{j,i,t})y_{j,i,t}I_{j,i,t}B_{j,i,t}\right] = 1 \\
\Leftrightarrow\; &\mathbb{E}_t\left[(r - r_{j,i,t})y_{j,i,t}I_{j,i,t}\right]\frac{\beta_\lambda \exp(-\beta_\lambda(s_{i,j,t} - \alpha_\lambda))}{\left(1+\exp(-\beta_\lambda(s_{i,j,t} - \alpha_\lambda))\right)^2} = 1
\end{aligned}$$

where the first step uses the definition of $l_{j,i,t}$, and the second step uses the independence of $B_{j,i,t}$. The above equation can be solved analytically for $s_{i,j,t}$ leading to Eq. (10).

The first-order condition for monitoring in Eq. (13) is

$$1 = \frac{1}{1+r^d}\frac{\partial \xi_{i,j,t}}{\partial m_{i,j,t}}\mathbb{E}_t\left(\frac{\frac{\partial \xi_{i,j,t+1}}{\partial \tilde{\sigma}^2_{i,j,t+1}}}{\frac{\partial \xi_{i,j,t+1}}{\partial m_{i,j,t+1}}} - \frac{\partial \pi_{i,j,t+1}}{\partial \tilde{\sigma}^2_{i,j,t+1}}\right).$$

Using the product rule, we get $\frac{\partial \pi_{i,j,t}}{\partial \tilde{\sigma}^2_{i,j,t}} = \frac{\partial \bar{R}_{i,j,t}}{\partial \tilde{\sigma}^2_{i,j,t}}y_{i,j,t}l_{i,j,t} + \bar{R}_{i,j,t}y_{i,j,t}B_{i,j,t}\frac{\partial I_{i,j,t}}{\partial \tilde{\sigma}^2_{i,j,t}}$, which we can further unfold using the following partial derivatives

$$\begin{aligned}
&\frac{\partial \phi_{i,j,t}}{\partial m_{i,j,t}} = \beta_\phi, \quad \frac{\partial P_{i,j,t}}{\partial \tilde{\sigma}^2_{i,j,t}} = \frac{\epsilon^2}{(\sigma^2 + \tilde{\sigma}^2_{i,j,t} + \epsilon^2)^2}, \quad \frac{\partial r_{i,j,t}}{\partial \tilde{\sigma}^2_{i,j,t}} = 0.5/\epsilon^2 \\
&\frac{\partial \xi_{i,j,t}}{\partial \phi_{i,j,t}} = \exp(\alpha_\sigma + \gamma_\sigma \log \tilde{\sigma}^2_{i,j,t} + \beta_\sigma \phi_{i,j,t} + \delta_\sigma u_{i,j,t})\beta_\sigma, \\
&\frac{\partial \xi_{i,j,t}}{\partial \tilde{\sigma}^2_{i,j,t}} = \exp(\alpha_\sigma + \gamma_\sigma \log \tilde{\sigma}^2_{i,j,t} + \beta_\sigma \phi_{i,j,t} + \delta_\sigma u_{i,j,t})/\tilde{\sigma}^2_{i,j,t}, \\
&\frac{\partial \bar{R}_{i,j,t}}{\partial \tilde{\sigma}^2_{i,j,t}} = -\frac{\partial P_{i,j,t}}{\partial \tilde{\sigma}^2_{i,j,t}} + \frac{\partial 1 - P_{i,j,t}}{\partial \tilde{\sigma}^2_{i,j,t}}r_{i,j,t} + (1 - P_{i,j,t})\frac{\partial r_{i,j,t}}{\partial \tilde{\sigma}^2_{i,j,t}} \\
&\frac{\partial I_{i,j,t}}{\partial \tilde{\sigma}^2_{i,j,t}} = \frac{\beta_I \exp(-\beta_I(r - r_{i,j,t}))}{1+\exp(-\beta_I(r - r_{i,j,t}))}\left(-\frac{\partial r_{i,j,t}}{\partial \tilde{\sigma}^2_{i,j,t}}\right).
\end{aligned}$$

Eq. (13) is highly nonlinear and does not have an analytical solution. We therefore follow the standard practice to compute an approximate solution based on a Taylor expansion. To this end, write the Euler equation more compactly as

$$\mathbb{E}_t f(m_{i,j,t}, \tilde{\sigma}^2_{i,j,t}, \tilde{\sigma}^2_{i,j,t+1}, B_{i,j,t+1}, y_{i,j,t+1}) = 0.$$

The local Taylor approximation of f requires an expansion point. The usual steady state (resulting from the absence of any shocks to the system) proves inappropriate in our setting, as steady state volumes would be zero and, as a consequence, the steady state corresponds to a critical point where all derivatives of f are zero. We therefore linearize the function f around the stable point $(\tilde{m}_{i,j}, \tilde{\tilde{\sigma}}^2_{i,j}, \tilde{\tilde{\sigma}}^2_{i,j}, \tilde{\lambda}_{i,j}, \tilde{y}_{i,j})$. This expansion point is obtained as the steady state of the system when $y_{i,j,t+1}$ is fixed at the expected loan volumes for two banks characterized by a liquidity shock distribution with mean parameter $\mathbb{E}(\mu_{\zeta^i}) = \mu_\mu$ and variance parameter $\mathbb{E}(\sigma^2_{\zeta^i}) = \exp(\mu_\sigma + \sigma^2_\sigma/2)$ (two "average" banks).[31] As a result the expansion point is the same for each bank pair (i, j).[32]

In the following expansion we write $h_x := \frac{\partial h(x,y)}{\partial x}$ and use $\hat{x} := x - \tilde{x}$ to denote a deviation from the expansion point. Applying the first-order Taylor expansion gives

$$f \approx \tilde{f} + f_{m_{i,j,t}} \hat{m}_{i,j,t} + f_{\tilde{\sigma}^2_{i,j,t}} \hat{\tilde{\sigma}}^2_{i,j,t} + f_{\tilde{\sigma}^2_{i,j,t+1}} \hat{\tilde{\sigma}}^2_{i,j,t+1} + f_{B_{i,j,t+1}} \hat{B}_{i,j,t+1} + f_{y_{i,j,t+1}} \hat{y}_{i,j,t+1}$$

where $\tilde{f} := f(\tilde{m}_{i,j}, \tilde{\tilde{\sigma}}^2_{i,j}, \tilde{\tilde{\sigma}}^2_{i,j}, \tilde{\lambda}_{i,j}, \tilde{y}_{i,j})$ and all derivatives are evaluated at the expansion point. Note that $\tilde{f} = 0$ by construction.

We then obtain the approximate Euler equation for monitoring as

$$\mathbb{E}_t\left[f_{m_{i,j,t}} \hat{m}_{i,j,t} + f_{\sigma^2_{i,j,t}} \hat{\tilde{\sigma}}^2_{i,j,t} + f_{\tilde{\sigma}^2_{i,j,t+1}} \hat{\tilde{\sigma}}^2_{i,j,t+1} + f_{B_{i,j,t+1}} \hat{B}_{i,j,t+1} + f_{y_{i,j,t+1}} \hat{y}_{i,j,t+1} \right] = 0,$$

which we rearrange to get the linear policy function,

$$m_{i,j,t} = a_m + b_m \tilde{\sigma}^2_{i,j,t} + c_m \mathbb{E}_t \tilde{\sigma}_{i,j,t+1} + d_m \mathbb{E}_t B_{i,j,t+1} + e_m \mathbb{E}_t y_{i,j,t+1},$$

that constitutes an approximate solution to the problem. Note that the intercept and the coefficients of the linear policy function are functions of the structural parameters.

Appendix B. Reduced form, stationarity, and ergodicity

Substituting the adaptive expectation mechanism in Eqs. (11) and (12) into the Euler equation for monitoring in (8) and the optimal search strategy in Eq. (9) allows us to re-write the full system in reduced form. The reduced form can be written as a nonlinear Markov autoregressive process,

$$\mathbf{X}_t = \mathbf{G}_{\boldsymbol{\theta}}(\mathbf{X}_{t-1}, \mathbf{e}_t),$$

where $\mathbf{G}_{\boldsymbol{\theta}}$ is a parametric vector function that depends on the structural model parameter $\boldsymbol{\theta}$, and $\mathbf{X}_t$ is the vector of all state-variables and control variables (observed or unobserved), and $\mathbf{e}_t$ is the vector of shocks driving the system. These shocks are the liquidity shocks $\{\zeta^i_{i,j,t}\}$, the bank-to-bank-specific shocks to the perception-error variance $\{u_{i,j,t}\}$, and the shocks that determine if a link between any two banks is open and trade is possible $\{B_{i,j,t}\}$. Obtaining the reduced-form representation is crucial as it allows us to simulate network paths for both state and control variables under a given structural parameter vector. Furthermore, this model formulation allows us to describe conditions for the strict stationarity and ergodicity of the model that are essential for the estimation theory that is outlined in Section 4.

Table B1
Lyapunov stability of the dynamic network model.

Parameter vector	$\boldsymbol{\theta}_0$	$\hat{\boldsymbol{\theta}}_T$
Lyapunov exponent	−0.6451	−0.2462

In particular, following Bougerol (1993), we find that under appropriate regularity conditions, the process $\{\mathbf{X}_t\}$ is strictly stationary and ergodic (SE).

Lemma 3. *For every $\boldsymbol{\theta} \in \Theta$, let $\{\mathbf{e}_t\}_{t\in\mathbb{Z}}$ be an SE sequence and assume there exists a (nonrandom) $\mathbf{x}$ such that $\mathbb{E}\log^+ \|\mathbf{G}_{\boldsymbol{\theta}}(\mathbf{x}, \mathbf{e}_t) - \mathbf{x}\| < \infty$ and suppose that the following contraction condition holds*

$$\mathbb{E}\ln \sup_{\mathbf{x}'\neq\mathbf{x}''} \frac{\|\mathbf{G}_{\boldsymbol{\theta}}(\mathbf{x}', \mathbf{e}_t) - \mathbf{G}_{\boldsymbol{\theta}}(\mathbf{x}'', \mathbf{e}_t)\|}{\|\mathbf{x}' - \mathbf{x}''\|} < 0. \tag{15}$$

Then the process $\{\mathbf{X}_t(\mathbf{x}_1)\}_{t\in\mathbb{N}}$, initialized at $\mathbf{x}_1$ and defined as

$$\mathbf{X}_1 = \mathbf{x}_1, \quad \mathbf{X}_t = \mathbf{G}_{\boldsymbol{\theta}}(\mathbf{X}_{t-1}, \mathbf{e}_t) \ \forall\ t \in \mathbb{N},$$

converges everywhere almost surely to a unique SE solution $\{\mathbf{X}_t\}_{t\in\mathbb{Z}}$ for every $\mathbf{x}_1$, that is $\|\mathbf{X}_t(\mathbf{x}_1) - \mathbf{X}_t\| \overset{e.a.s.}{\to} 0$ as $t \to \infty$.[33]

[31] Due to the normality assumption for the liquidity shocks we can compute $\tilde{y}_{i,j} := \mathbb{E}(y_{i,j,t})$ analytically. Given $\tilde{y}_{i,j}$ we solve for the steady state values of $\tilde{m}_{i,j}, \tilde{\tilde{\sigma}}^2_{i,j}, \tilde{\lambda}_{i,j}$ under the absence of shocks to $\tilde{\sigma}^2_{i,j}$.

[32] Computationally it is infeasible to compute $N(N-1)$ different expansion points depending on banks' liquidity distribution.

[33] A stochastic sequence $\{\xi_t\}$ is said to satisfy $\|\xi_t\| \overset{e.a.s.}{\to} 0$ if $\exists\, \gamma > 1$ such that $\gamma^t \|x_t\| \overset{a.s.}{\to} 0$.

The condition that $\mathbb{E}\log^{+}\|\mathbf{G}_{\boldsymbol{\theta}}(\mathbf{x},\mathbf{e}_t)-\mathbf{x}\|<\infty$ can be easily verified for any given distribution for the innovations $\mathbf{e}_t$ and any given shape function $\mathbf{G}_{\boldsymbol{\theta}}$. The contraction condition in Eq. (15) is, however, much harder to verify analytically.

Fortunately, the contraction condition can be re-written as

$$\mathbb{E}\log\sup_{\mathbf{x}}\|\nabla\mathbf{G}_{\boldsymbol{\theta}}(\mathbf{x},\mathbf{e}_t)\|<0 \tag{16}$$

where $\nabla\mathbf{G}_{\boldsymbol{\theta}}$ denotes the Jacobian of $\mathbf{G}_{\boldsymbol{\theta}}$ and $\|\cdot\|$ is a norm. By verifying numerically that this inequality holds at every step $\boldsymbol{\theta}\in\Theta$ of the estimation algorithm, one can ensure that the simulation-based estimation procedure has the appropriate stochastic properties.

The contraction condition of Bougerol (1993) in Eq. (16) essentially states that the maximal Lyapunov exponent must be negative uniformly in $\mathbf{x}$.

Definition 1. The maximal Lyapunov exponent is given by $\lim_{t\to\infty}\frac{1}{t}\log\max_i\Lambda_{i,t}=\mathbb{E}\log\max_i\Lambda_{i,t}$ where $\Lambda_{i,t}$'s are eigenvalues of the Jacobian matrix $\nabla\mathbf{G}_{\boldsymbol{\theta}}(\mathbf{x}_t,\mathbf{e}_t)$.

A negative Lyapunov exponent ensures the stability of the network paths. Appendix Table 1 uses the Jacobian of the structural dynamic system $\mathbf{G}_{\boldsymbol{\theta}}(\mathbf{x},\mathbf{e}_t)$ to report numerical calculations of the maximal Lyapunov exponent of our dynamic stochastic network model at the parameters $\boldsymbol{\theta}_0$ and $\hat{\boldsymbol{\theta}}_T$ described in Table 3 of Section 4.3. These points in the parameter space correspond to the starting point for the estimation procedure described in Section 4 and the final estimated point.

Despite the higher degree of persistence at $\hat{\boldsymbol{\theta}}_T$ compared to $\boldsymbol{\theta}_0$ (a higher Lyapunov exponent), the contraction condition is satisfied in both cases as the maximal Lyapunov exponent is negative. This ensures that both $\boldsymbol{\theta}_0$ and $\hat{\boldsymbol{\theta}}_T$ generate stable network paths.

Appendix C. Network auxiliary statistics

In this section, we provide formulæ for the non-standard auxiliary statistics that characterize specifically the (dynamic) structure of the interbank lending network. First, the global network statistics that relate to the sparsity, reciprocity and stability are given as

$$density_t=\frac{1}{N(N-1)}\sum_{i,j}l_{i,j,t},\quad reciprocity_t=\frac{\sum_{i,j}l_{i,j,t}l_{j,i,t}}{\sum_{i,j}l_{i,j,t}},$$

$$stability_t=\frac{\sum_{i,j}\left(l_{i,j,t}l_{i,j,t-1}+(1-l_{i,j,t})(1-l_{i,j,t-1})\right)}{N(N-1)}.$$

Further, we maintain information about the *degree distribution*. In the interbank market, the degree centrality of a bank counts the number of different trading partners. For directed networks the out- and in-degree of node i are given by

$$d^{out}_{i,t}=\sum_j l_{i,j,t}\quad\text{and}\quad d^{in}_{i,t}=\sum_j l_{j,i,t}.$$

Instead of considering all $2N$ variables individually, we consider the mean, variance and skewness of the out-degree and in-degree distribution. The mean of degree distribution is proportional to the density. In the estimation procedure we include therefore only the average degree.

The (local) clustering coefficient of node i in a binary unweighted network is given by

$$c_{i,t}=\frac{1/2\sum_j\sum_h(l_{i,j,t}+l_{j,i,t})(l_{i,h,t}+l_{h,i,t})(l_{j,h,t}+l_{h,j,t})}{d^{tot}_{i,t}(d^{tot}_{i,t}-1)-2d^{\leftrightarrow}_{i,t}},$$

where $d^{tot}_{i,t}=d^{in}_{i,t}+d^{out}_{i,t}$ is the total degree and $d^{\leftrightarrow}_{i,t}=\sum_{j\neq i}l_{i,j,t}l_{j,i,t}$ (see Fagiolo, 2007). We consider the average clustering coefficient, defined as the mean of the local clustering coefficients.

Second, we compute simple bilateral local network statistics that measure the intensity of a bilateral trading relationship based on a rolling window of size $T_{rw}=5$ (one five-day business week). As a simple measure of bilateral relationships, we compute the number of loans given from bank i to bank j during periods $t'=\{t-T_{rw}+1,\dots,t\}$ and denote this variable by

$$l^{rw}_{i,j,t}=\sum_{t'}l_{i,j,t'},$$

where the sum runs over $t'=\{t-T_{rw}+1,\dots,t\}$. We then consider for each t the correlation between current access and past trading intensity, and between current interest spreads (for granted) loans and past trading intensity,

$$\mathrm{Corr}(l_{i,j,t},l^{rw}_{i,j,t})\text{ and }\mathrm{Corr}(r_{i,j,t},l^{rw}_{i,j,t}).$$

All described network statistics are computed for the network of interbank lending at each time period t such that we obtain a sequence of network statistics. We then obtain the unconditional means, variance and/or autocorrelation of these sequences as auxiliary statistics and base the parameter estimations on the values of the auxiliary statistics only.

Appendix D. Additional results on econometric properties

D1. Discussion of sensitivity analysis

A closer look at the response of the sensitivity analysis of the auxiliary statistics to changes in the structural parameters presented in Fig. 2 reveals further insights about the model mechanics.

In the left panel, we see that an increase in the persistence of the log perception-error variance leads to a lower network density and a higher fraction of reciprocal lending relationships. Moreover, for the plotted range of values of γ_σ, both the in- and out-degree skewness exhibit a hump shaped form. For a low persistence in credit-risk uncertainty, an initial increase in γ_σ leads to higher skewness of the degree distributions, in particular the in-degree becomes more asymmetrically distributed. Economically, as the persistence of credit-risk uncertainty increases, some banks lose trading partners—which potentially cuts off their access to the interbank market—while few highly connected banks can still maintain sufficiently many lending relations (these money center banks are intensively monitored, as they are frequent large-volume borrowers). As the uncertainty increases further, however, lender banks will also occasionally refrain from providing credit to money center banks, and the skewness decreases again. In addition, more persistent uncertainty leads to higher spreads of granted loans and decreases monitoring efforts due to lower profitability.

The network shows a qualitatively similar response to a local increase in the marginal effect of monitoring on the added information; specifically, the density decreases and lending becomes more reciprocal (center panel). At the same time, the average spread of granted loans increases and banks on average reduce peer monitoring efforts (bottom plot). The decline in monitoring occurs because $\frac{\partial \pi_{i,t}}{\partial m_{i,j,t} \partial \beta_{\phi,1}}|_{\theta=\hat{\theta}} < 0$ for sufficiently large $m_{i,j,t}$, in particular at the expansion point of the first order conditions. Intuitively, banks' steady-state monitoring levels are such that uncertainty is already relatively low, and an increase in $\beta_{\phi,1}$ further reduces the marginal benefits from monitoring. To maintain the equality between the (constant) marginal cost and benefit, it is necessary to reduce monitoring efforts. The results confirm our findings where we compare the results for the estimated model with those for a model without monitoring ($\beta_{\phi,1} = 0$).

The right panel reveals that if banks need to invest more to maintain the same link probability, less trading occurs and lending becomes less reciprocal because some banks will not find it profitable to maintain some of their trading relationships. However, as the large increase in the in-degree skewness suggests, at the borrower level, the reduction in lending partners is again asymmetrically distributed. In particular, as the cost of link formation increases, borrowing becomes more concentrated toward few highly connected core banks. At the same time, the reduction in out-degree skewness reflects that highly connected lenders lose some of their borrowers that do not find it profitable anymore to incur the search cost, thereby reducing the asymmetry of the degree distribution. Moreover, while the average monitoring expenditures decrease as a reaction to the higher cost of linking, the mean spread of granted loans decreases because those bank pairs that continue trading have lower uncertainty about their counterparts.

Table D1
Finite-sample distribution of estimator under incorrect specification.

DGP:	Time-varying bargaining power				Common uncertainty shock				Without monitoring			
	θ_0	mean($\hat{\theta}$)	p50($\hat{\theta}$)	RMSE($\hat{\theta}$)	θ_0	mean($\hat{\theta}$)	p50($\hat{\theta}$)	RMSE($\hat{\theta}$)	θ_0	mean($\hat{\theta}$)	p50($\hat{\theta}$)	RMSE($\hat{\theta}$)
$\beta_{\phi,1}$	9.6000	9.7353	9.6713	0.7257	9.6000	9.4325	9.4867	1.0387	–	0.0837	0.0633	–
$\beta_{\phi,2}$	1.00E-04	1.01E-04	1.01E-04	6.57E-06	1.00E-04	1.02E-04	1.00E-04	1.38E-05	1.0001	0.998637	1.0001	0.11118
α_σ	1.2890	1.3030	1.3009	0.1187	1.2890	1.3116	1.2961	0.1130	1.2890	1.3129	1.2890	0.1329
γ_σ	0.6648	0.6622	0.6670	0.0381	0.6648	0.8064	0.7623	0.2061	0.6648	0.5038	0.6573	0.3034
δ_σ	0.3383	0.3400	0.3383	0.0317	0.3383	0.3832	0.3704	0.0755	0.3383	0.3478	0.3383	0.0325
α_λ	1.00E-04	9.96E-05	1.00E-04	1.11E-05	1.00E-04	9.99E-05	1.00E-04	1.77E-05	1.00E-04	1.03E-04	1.00E-04	1.24E-05
β_λ	72.8331	73.9452	73.2277	7.1368	72.8331	75.7237	72.8331	15.9748	72.8331	72.5953	72.8331	7.7337
σ^*_μ	1.9903	2.0449	2.0264	0.2129	1.9903	2.3383	2.2342	0.5305	1.9903	1.9511	1.9903	0.2180
μ_σ	1.9492	1.8243	1.8642	0.2513	1.9492	1.8863	1.8973	0.2745	1.9492	2.0092	1.9514	0.2798
σ_σ	1.9810	2.0712	1.9895	0.3031	1.9810	2.0181	1.9810	0.3119	1.9810	2.0599	1.9843	0.2715
ρ_ζ	0.7826	0.7811	0.7867	0.0842	0.7826	0.6715	0.6967	0.1991	0.7826	0.8227	0.8113	0.1045
λ_B	0.9278	0.9190	0.9381	0.0937	0.9278	0.9147	0.9278	0.0747	–	0.9214	0.9278	–
λ_y	0.8472	0.8580	0.8768	0.1299	0.8472	0.8583	0.8534	0.1064	0.8472	0.8568	0.8475	0.0842
λ_r	0.4008	0.4058	0.4019	0.0442	0.4008	0.3982	0.4008	0.0817	0.4008	0.4082	0.4008	0.0324
$\lambda_{\bar{\sigma}}$	0.0318	0.0326	0.0321	0.0034	0.0318	0.0316	0.0318	0.0035	–	0.0326	0.0318	–
θ	–	0.6574	0.6759	–	0.6896	0.4142	0.2834	0.4140	0.4896	0.5055	0.4896	0.0528

Notes: The table reports key statistics of the finite-sample distribution for the indirect inference network estimator. Results are based on a Monte Carlo study with 250 repetitions, where the data are generated under different parametrization with $N = 50$ and $T = 1000$, and $S = 24$ network paths. Under the parametrization "Time-Varying Bargaining Power" the bargaining power parameter follows a logistic transformation of an AR process; under "Common Uncertainty Shock" introduces a common shock to credit-risk uncertainty; "Without Monitoring" generates data under a parametrization without monitoring. The root mean squared error (RMSE) is only shown for parameters that are present both in the DGB and in the estimated model. Calibrated parameters are similar to Table 3. See text for details.

D2. Finite-sample distribution under misspecification

Given that our structural network model is likely to be misspecified, i.e., the data generating process is different than postulated by the proposed model, we analyze in this section the finite-sample performance of the estimator under misspecification. We consider different data generating processes that include cases of misspecification that could correspond to empirically relevant situations in our application. First, we consider time-variation in the bargaining parameter modeled as a logistic transformation of an autoregressive process: $\theta_t = \frac{\exp(\alpha_{\theta,t})}{1+\exp(\alpha_{\theta,t})}$, where $\alpha_{\theta,t+1} = 0.95\alpha_{\theta,t} + 0.2\epsilon_{\theta,t}$ and $\epsilon_{\theta,t} \sim \mathcal{N}(0,1)$. Time variation in bargaining power is likely to have shifted with different monetary policy changes in the aftermath of Lehman's failure (e.g., the ECB full-allotment policy, the long-term refinancing operations, etc.). Second, in addition to bank-pair-specific shocks, we introduce a common shocks to the perception error variance. In terms of Eq. (1), $u_{i,j,t} = \sqrt{0.5}u^1_{i,j,t} + \sqrt{0.5}u^2_t$, where both the idiosyncratic shock $u^1_{i,j,t}$ and the common shock u^2_t are independently and standard normally distributed. This situation may be relevant, for example, in the context of the financial crisis, when general uncertainty was high. Finally, we consider an alternative model parametrization where monitoring has no effect on the credit-risk uncertainty to analyze if the estimator would pick up the zero coefficient ($\beta_{\phi,1} = 0$), or whether it would falsely attribute an effect to monitoring.

For each of these cases, we estimate the full model as outlined in the main body of the text, that is, the model is misspecified with respect to the true data generating process. The results are presented in Appendix Table 2, which presents the parameters used under simulation (a dash indicates that the parameter does not exist in the DGP under consideration), the mean and median of the small sample distribution of the estimated parameters, and, if applicable, the RMSE. All parameters of the MC are similar to the previous MC study. Our main focus is how the model misspecification affects the parameter estimates of the effectiveness of monitoring. First, the results show that misspecification introduces a larger bias in the estimator compared to the case of correct specification, and the finite sample distribution widens. Indeed, the RMSEs for $\beta_{\phi,1}$ are about 22% (DGP with time-varying bargaining power) and 75% (DGP with common uncertainty shock) larger than under correct specification. Second, however, despite the larger bias and wider dispersion introduced by the misspecification, the small-sample distribution is still reasonably well centered around the parameter values used for simulation as for most parameters the mean and median are close to the values used to generate the data. Third, when we simulate data from the model under the constraint that monitoring has no effect on credit risk uncertainty ($\beta_{\phi,1} = 0$), we find that the estimator is also centered close to zero.

Appendix E. Parameter estimates for subsamples

Table E1
Parameter estimates for subsamples.

		Before Lehman failure (1)	After Lehman failure (2)
Added information	$\beta_{\phi,1}$	5.3824	8.6419
	$\beta_{\phi,2}$	0.0001	0.0001
Preception error variance	α_σ	1.0403	1.3412
	γ_σ	0.7183	0.6798
	δ_σ	0.369	0.0788
Search technology	α_λ	0.0001	0.0001
	β_λ	81.6715	78.7337
Liquidity shocks	σ^*_μ	2.0341	2.0412
	μ_σ	1.8371	1.8221
	σ_σ	2.587	1.9958
	ρ_ξ	−0.8245	−0.3972
Expectations	λ^β	0.7918	0.9898
	λ^y	0.9933	0.927
	λ^r	0.4367	0.2944
	$\lambda^{\tilde{\sigma}}$	0.0249	0.0323
Bargaining power	θ	0.7455	0.7374

Notes: This table reports the estimated structural parameters of the model, $\hat{\boldsymbol{\theta}}_T$, for two subsamples: (1) for the period before Lehman's failure from February 18, 2008, through September, 12, 2008, and (2) for the period after Lehman's failure from September 15, 2008, through December 1, 2008. The indirect inference estimator is based on $S = 24$ simulated network paths, each of length 3,000 periods. Calibrated parameters are similar to Table 3. Note also that $\sigma^*_\mu = \log(\sigma_\mu)$.

References

Acemoglu, D., Ozdaglar, A., Tahbaz-Salehi, A., 2015. Systemic risk and stability in financial networks. Am. Econ. Rev. 105 (2), 564–608.

Acharya, V.V., Merrouche, O., 2013. Precautionary hoarding of liquidity and interbank markets: evidence from the subprime crisis. Rev. Financ. 17 (1), 107–160. http://ideas.repec.org/a/oup/revfin/v17y2013i1p107-160.html.

Affinito, M., 2012. Do interbank customer relationships exist? And how did they function over the crisis? Learning from Italy. J. Bank. Financ. 36 (12), 3163–3184.

Afonso, G., Kovner, A., Schoar, A., 2011. Stressed, not frozen: the federal funds market in the financial crisis. J. Financ. 66 (4), 1109–1139. http://ideas.repec.org/a/bla/jfinan/v66y2011i4p1109-1139.html.

Afonso, G., Kovner, A., Schoar, A., 2013. Trading Partners in the Interbank Lending Market. Staff Reports 620. Federal Reserve Bank of New York. http://EconPapers.repec.org/RePEc:fip:fednsr:620.

Afonso, G., Lagos, R., 2015. Trade dynamics in the market for federal funds. Econometrica 83 (1), 263–313.

Allen, F., Gale, D., 2000. Financial contagion. J. Political Econ. 108 (1), 1–33. http://ideas.repec.org/a/ucp/jpolec/v108y2001i1p1-33.html.

Anand, K., van Lelyveld, I., Banai, A., Christiano Silva, T., Friedrich, S., Garratt, R., Halaj, G., Hansen, I., Howell, B., Lee, H., Martínez Jaramillo, S., Molina-Borboa, J.L., Nobili, S., Rajan, S., Rubens Stancato de Souza, S., Salakhova, D., Silvestri, L., 2018. The missing links: a global study on uncovering financial network structure from partial data. J. Financ. Stab. in press.

Arciero, L., Heijmans, R., Heuver, R., Massarenti, M., Picillo, C., Vacirca, F., 2013. How to measure the unsecured money market? The Eurosystem's implementation and validation using TARGET2 data. Working Paper 369. De Nederlandsche Bank, Amsterdam.

Ashcraft, A.B., Duffie, D., 2007. Systemic illiquidity in the federal funds market. Am. Econ. Rev. 97 (2), 221–225. http://www.jstor.org/stable/30034450.

Babus, A., 2013. Endogenous Intermediation in Over-the-Counter Markets. Unpublished working paper.

Bech, M.L., Atalay, E., 2010. The topology of the federal funds market. Phys. A: Stat. Mech. Appl. 389 (22), 5223–5246. http://ideas.repec.org/a/eee/phsmap/v389y2010i22p5223-5246.html.

Bech, M.L., Klee, E., 2011. The mechanics of a graceful exit: interest on reserves and segmentation in the federal gunds market. J. Monet. Econ. 58 (5), 415–431. http://ideas.repec.org/a/eee/moneco/v58y2011i5p415-431.html.

Bech, M.L., Monnet, C., 2013. The impact of unconventional monetary policy on the overnight interbank market. In: Heath, A., Lilley, M., Manning, M. (Eds.), Liquidity and Funding Markets. Reserve Bank of Australia, Sydney. RBA Annual Conference Volume.

Becher, C., Millard, S., Soramäki, K., 2008. The Network Topology of CHAPS Sterling. Working Paper 355. Bank of England, London. http://ideas.repec.org/p/boe/boeewp/0355.html.

Berentsen, A., Monnet, C., 2008. Monetary policy in a channel system. J. Monet. Econ. 55 (6), 1067–1080. http://ideas.repec.org/a/eee/moneco/v55y2008i6p1067-1080.html.

Bindseil, U., Jabłecki, J., 2011. The Optimal Width of the Central Bank Standing Facilities Corridor and Banks' Day-to-Day Liquidity Management. Working Paper Series 1350. European Central Bank, Frankfurt. http://ideas.repec.org/p/ecb/ecbwps/20111350.html.

Blasques, F., Duplinskiy, 2018. Penalized indirect inference. J. Econo. in press.

Boss, M., Elsinger, H., Summer, M., Thurner, S., 2004. Network topology of the interbank market. Quant. Financ. 4 (6), 677–684. http://ideas.repec.org/a/taf/quantf/v4y2004i6p677-684.html.

Bougerol, P., 1993. Kalman filtering with random coefficients and contractions. SIAM J. Control Optim. 31 (4), 942–959. doi:10.1137/0331041.

Bräuning, F., Fecht, F., 2017. Relationship lending in the interbank market and the price of liquidity. Rev. Financ. 21 (1), 33–75. https://ideas.repec.org/a/oup/revfin/v21y2017i1p33-75.html.

Chow, G.C., 1989. Rational versus adaptive expectations in present value models. Rev. Econ. Stat. 71 (3), 376–384. http://ideas.repec.org/a/tpr/restat/v71y1989i3p376-84.html.

Chow, G.C., 2011. Usefulness of Adaptive and Rational Expectations in Economics. Working Paper 1334. Department of Economics, Center for Economic Policy Studies, Princeton University, Princeton, NJ. http://EconPapers.repec.org/RePEc:pri:cepsud:221chow.

Cocco, J.F., Gomes, F.J., Martins, N.C., 2009. Lending relationships in the interbank market. J. Financ. Intermediation 18 (1), 24–48.

Cœuré, B., 2013. Exit strategies: time to think about them. Proceedings of Speech at the 15th Geneva Conference on the World Economy, http://http://www.ecb.europa.eu/press/key/date/2013/html/sp130503.en.html, Accessed on August 22, 2014.

Craig, B., von Peter, G., 2014. Interbank tiering and money center banks. J. Financ. Intermediation 23 (3), 322–347. https://doi.org/10.1016/j.jfi.2014.02.003. http://www.sciencedirect.com/science/article/pii/S1042957314000126.

Davidson, R., MacKinnon, J. G., 1993. Estimation and Inference in Econometrics. OUP Catalogue.

DeJong, D.N., Dave, C., 2006. Structural Macroeconometrics. Princeton University Press, Princeton, NJ.

Diamond, D.W., Dybvig, P.H., 1983. Bank runs, deposit insurance, and liquidity. J. Political Econ. 91 (3), 401–419. http://ideas.repec.org/a/ucp/jpolec/v91y1983i3p401-19.html.

Duffie, D., Garleanu, N., Pedersen, L.H., 2005. Over-the-counter markets. Econometrica 73 (6), 1815–1847. http://ideas.repec.org/a/ecm/emetrp/v73y2005i6p1815-1847.html.

Evans, G.W., Honkapohja, S., 2001. Learning and Expectations in Macroeconomics. Princeton University Press, Princeton, NJ.

Fagiolo, G., 2007. Clustering in complex directed networks. Phys. Rev. E 76, 026107. doi:10.1103/PhysRevE.76.026107.

Farboodi, M., 2014. Intermediation and Voluntary Exposure to Counterparty Risk. Unpublished working paper.

Fecht, F., Nyborg, K.G., Rocholl, J., 2011. The price of liquidity: the effects of market conditions and bank characteristics. J. Financ. Econ. 102 (2), 344–362.

Freixas, X., Holthausen, C., 2005. Interbank market integration under asymmetric information. Rev. Financ. Stud. 18 (2), 459–490. http://www.jstor.org/stable/3598043.

Freixas, X., Jorge, J., 2008. The role of interbank markets in monetary policy: a model with rationing. J. Money Credit Bank. 40 (6), 1151–1176. http://ideas.repec.org/a/mcb/jmoncb/v40y2008i6p1151-1176.html.

Furfine, C.H., 1999. The microstructure of the federal funds market. Financ. Mark. Inst. Instrum. 8 (5), 24–44.

Furfine, C.H., 2001. Banks as monitors of other banks: evidence from the overnight federal funds market. J. Bus. 74 (1), 33–57.

Gabrieli, S., Georg, C.-P., 2014. A Network View on Money Market Freezes. Mimeo.

Gai, P., Haldane, A., Kapadia, S., 2011. Complexity, concentration and contagion. J. Monet. Econ. 58 (5), 453–470. http://ideas.repec.org/a/eee/moneco/v58y2011i5p453-470.html.

Gale, D.M., Kariv, S., 2007. Financial networks. Am. Econ. Rev. 97 (2), 99–103. http://www.jstor.org/stable/30034428.

Georg, C.-P., 2013. The effect of the interbank network structure on contagion and financial stability. J. Bank. Financ. 77 (7), 2216–2228.

Gofman, M., 2014. Efficiency and Stability of a Financial Architecture with Too-Interconnected-to-Fail Institutions. Unpublished working paper.

Gourieroux, C., Monfort, A., Renault, E., 1993. Indirect inference. J. Appl Econom. 8 (S), S85–118. http://ideas.repec.org/a/jae/japmet/v8y1993isps85-118.html.

Grazzini, J., Richiardi, M., Collegio, C., Alberto, C., Revelli, L., 2014. Estimation of Ergodic agent-based models by simulated minimum distance. J. Econ. Dyn. Control 51, 148–165. https://www.nuffield.ox.ac.uk/media/1690/abmestimation-ergodicv18.pdf.

Heer, B., Maußner, A., 2005. Dynamic General Equilibrium Modelling. Springer, Berlin.

Heider, F., Hoerova, M., Holthausen, C., 2015. Liquidity hoarding and interbank market spreads: the role of counterparty risk. J. Financ. Econ. 118 (2), 336–454.

Heijmans, R., Heuver, R., Walraven, D., 2011. Monitoring the Unsecured Interbank Money Market Using TARGET2 Data. Working Paper Series 276. De Nederlandsche Bank, Amsterdam. http://ideas.repec.org/p/dnb/dnbwpp/276.html.

Hoff, P.D., Raftery, A.E., Handcock, M.S., 2002. Latent space approaches to social network analysis. J. Am. Stat. Assoc. 97 (460), 1090–1098.

Iori, G., Masi, G.D., Precup, O.V., Gabbi, G., Caldarelli, G., 2008. A network analysis of the Italian overnight money market. J. Econ. Dyn. Control 32 (1), 259–278.
Jackson, M.O., 2008. Social and Economic Networks. Princeton University Press, Princeton, NJ.
Judd, K.L., 1998. Numerical Methods in Economics. The MIT Press, Cambridge, MA.
Kolaczyk, E.D., 2009. Statistical Analysis of Network Data: Methods and Models, first ed. Springer Publishing Company, Incorporated.
Lux, T., Fricke, D., 2012. Core-Periphery Structure in the Overnight Money Market: Evidence from the e-MID Trading Platform. Kiel Working Paper 1759. Kiel Institute for the World Economy, Kiel. http://ideas.repec.org/p/kie/kieliw/1759.html.
May, R.M., Levin, S.A., Sugihara, G., 2008. Complex systems: ecology for bankers. Nature 451 (7181), 893–895. doi:10.1038/451893a.
Poole, W., 1968. Commercial bank reserve management in a stochastic model: implications for monetary policy. J. Financ. 23 (5), 769–791. http://ideas.repec.org/a/bla/jfinan/v23y1968i5p769-791.html.
Rochet, J.-C., Tirole, J., 1996. Interbank lending and systemic risk. J. Money Credit Bank. 28 (4), 733–762. http://www.jstor.org/stable/2077918.
Ruge-Murcia, F.J., 2007. Methods to estimate dynamic stochastic general equilibrium models. J. Econ. Dyn. Control 31 (8), 2599–2636. http://ideas.repec.org/a/eee/dyncon/v31y2007i8p2599-2636.html.
Snijders, T.A., van de Bunt, G.G., Steglich, C.E., 2010. Introduction to stochastic actor-based models for network dynamics. Soc. Netw. 32 (1), 44–60. doi:10.1016/j.socnet.2009.02.004. Dynamics of Social Networks. https://www.sciencedirect.com/science/article/pii/S0378873309000069.
Soramäki, K., Bech, M.L., Arnold, J., Glass, R.J., Beyeler, W.E., 2007. The topology of interbank payment flows. Phys. A: Stat. Mech. Appl. 379 (1), 317–333. http://ideas.repec.org/a/eee/phsmap/v379y2007i1p317-333.html.
Stock, J.H., Wright, J.H., 2000. GMM with weak identification. Econometrica 68 (5), 1055–1096.
in 't Veld, D., van der Leij, M., Hommes, C., 2014. The Formation of a Core Periphery Structure in Heterogeneous Financial Networks. Tinbergen Institute Discussion Paper 14-098/II. Tinbergen Institute, Amsterdam. http://ideas.repec.org/p/dgr/uvatin/20140098.html.
in 't Veld, D., van Lelyveld, I., 2014. Finding the core: network structure in interbank markets. J. Bank. Financ. 49 (December), 27–40.
Vuillemey, G., Breton, R., 2014. Endogenous Derivative Networks. Working Paper 483. Banque de France, Paris.
White, H., 2001. Asymptotic Theory for Econometricians. Academic Press, Orlando, FL. Revised Edition.
Whitesell, W., 2006. Interest rate corridors and reserves. J. Monet. Econ. 53 (6), 1177–1195. http://ideas.repec.org/a/eee/moneco/v53y2006i6p1177-1195.html.